University of South Carolina
Scholar Commons

Theses and Dissertations

1-1-2013

Thermal History of Nearly Metamict Zircon of the Taza-Guercif Basin (Morocco) Revealed Using Scanning Electron Microscope High-Density Fission-Track Dating

Tyler Michael Izykowski
University of South Carolina - Columbia

Follow this and additional works at: https://scholarcommons.sc.edu/etd

 Part of the Earth Sciences Commons

Recommended Citation

Izykowski, T. M.(2013). *Thermal History of Nearly Metamict Zircon of the Taza-Guercif Basin (Morocco) Revealed Using Scanning Electron Microscope High-Density Fission-Track Dating.* (Doctoral dissertation). Retrieved from https://scholarcommons.sc.edu/etd/2460

This Open Access Dissertation is brought to you by Scholar Commons. It has been accepted for inclusion in Theses and Dissertations by an authorized administrator of Scholar Commons. For more information, please contact dillarda@mailbox.sc.edu.

www.manaraa.com

THERMAL HISTORY OF NEARLY METAMICT ZIRCON OF THE TAZA-GUERCIF BASIN (MOROCCO) REVEALED USING SCANNING ELECTRON MICROSCOPE HIGH-DENSITY FISSION-TRACK DATING

by

Tyler Michael Izykowski

Bachelor of Science
Union College, 2011

Submitted in Partial Fulfillment of the Requirements

For the Degree of Master of Science in

Geological Sciences

College of Arts and Sciences

University of South Carolina

2013

Accepted by:

David L. Barbeau, Jr., Director of Thesis

James H. Knapp, Reader

Gene M. Yogodzinski, Reader

Lacy Ford, Vice Provost and Dean of Graduate Studies

www.manaraa.com

© Copyright by Tyler Izykowski, 2013
All Rights Reserved.

www.manaraa.com

DEDICATION

This thesis is dedicated to my parents, Denise and Thomas, for their continued support of my academic and life pursuits.

www.manaraa.com

ACKNOWLEDGEMENTS

I would like to thank the following people and organizations, without which this work could not have been completed: The University of South Carolina Department of Earth and Ocean Sciences for embracing and supporting the maiden field season of this project; Université Mohammed V Agdal Institut Scientique de Rabat for providing travel support and insight in the field; Union College for allowing access to their Fission Track Laboratory and Zeiss EVO50 scanning electron microscope; Oregon State University for conducting neutron irradiation in their TRIGA Mark II Research Reactor (OSTR); the National Science Foundation for providing funding through grants awarded to Dr. David Barbeau (NSF 0732995, NSF 1241460), Dr. John Garver (NSF EAR 1116554, NSF EAR 0619578), and Dr. Cameron Davidson (NSF EAR 1116536); and the Geological Society of America for funding awarded to Jonathan Pratt (Ph.D candidate, University of South Carolina). Without the insight and logistical support of professors David Barbeau (University of South Carolina), John Garver (Union College), Anas Emran and Juadi (Université Mohammed V Agdal), as well as my committee members, Drs. James Knapp and Gene Yogodzinski, this project would not have been possible. This project is part of a larger ongoing project originally proposed and organized by Jonathan Pratt.

www.manaraa.com

ABSTRACT

Northwest Africa provides unique insight into a wide range of geologic processes throughout a vast portion of Earth's history. Moroccan geology in particular can provide valuable insight, from the formations of West Africa through the Eburnian orogeny (~2000 Ma), Gondwana during the Pan-African orogeny (~900-500 Ma), and Pangaea by means of the Hercynian (Variscan) orogeny (~400-300 Ma), to more recent crustal and climatic events, such as the Messinian salinity crisis (5.96-5.33 Ma). However, the current lack of western literature regarding this region presents a significant obstacle in understanding the aforementioned processes. Herein, I employ a new technique in zircon fission-track dating, a thermochronological tool that has proved integral in understanding tectonic and sedimentary systems, in order to provide new insight into the ancient and recent geologic past of northern Morocco.

Standard zircon fission-track dating is a powerful tool for understanding source-to-sink systems; that is, the tracing of sediment from its original source, or provenance, through initial erosion, ensuing transport, and ultimate deposition in sedimentary basins. However, conventional, optically based fission-track analysis has historically been limited in application due to the densities of fission-tracks that can be counted with the ~1500x magnification ceiling of optical microscopes. Standard fission-track dating has an upper limit of approximately 2 x 10^7 tracks/cm^2, making it difficult to analyze very old

www.manaraa.com

and very high-uranium content zircon grains. The present advancement in fission-track analysis incorporates the increased magnification of scanning electron microscopy to reconstruct the long-term thermal history of basin sediments of the Taza-Guercif basin, located in the South Rifean Corridor of Morocco. Highly damaged zircon grains were selected to evaluate the low temperature (~200-300°C) thermal histories of basin sediments as well as the two most proximal and likely sediment sources. Two significant cooling age populations were revealed at 607 Ma and 319 Ma, likely relating to the Pan-African and Hercynian Orogenies, respectively. The absence of a more recent cooling age population suggests a relatively long period (at least 300 Myr) of thermal quiescence in the Western Mediterranean, despite being in an active convergence zone with numerous tectonothermal events, namely Neogene Betic-Rif Alpine metamorphism.

www.manaraa.com

Table of Contents

www.manaraa.com

LIST OF TABLES

www.manaraa.com

LIST OF FIGURES

www.manaraa.com

List of Abbreviations

PAZ ..... Partial Annealing Zone

SEM ..... Scanning Electron Microscope

SEM-HDFT ..... Scanning Electron Microscopy High-Density Fission-Track

ZFT ..... Zircon Fission-Track

www.manaraa.com

CHAPTER 1

INTRODUCTION

Since its inception over four decades ago, fission-track dating has emerged and developed into one of the most beneficial tools for understanding source-to-sink systems, or the processes by which sediment is initially created through weathering and eventually deposited in a basin (Price & Walker, 1963; Fleisher et al., 1975; Tagami & O'Sullivan, 2005). While geochronology techniques such as U/Pb dating are useful in determining crystallization histories and sediment provenance (Gehrels et al., 1995), they are limited in that they generally do not record post-crystallization thermal history, as the closure temperature for the system is ~900°C (Reiners et al., 2005). In contrast, thermochronological dating methods such as fission-track and helium dating allow for the dating of low-temperature thermal events in uranium-bearing minerals, making them very useful in understanding exhumation and burial histories (Montario & Garver, 2009), and providing an additional provenance tool (Hurford & Carter, 1991; also, see discussion in Bernet & Garver, 2005). While similar analyses are also commonly employed on the phosphate apatite, fission-track and helium dating are generally more effectively employed on zircon ($ZrSiO_4$) in sediments and sedimentary rocks, due to the silicate's greater chemical and physical resistance to weathering. While zircon (U-Th)/He (ZHe dating) accesses a lower temperature component of thermal history (180 ± 20°C; Reiners et al., 2003), it also requires the complete dissolution of the zircon grain, rendering additional analyses impossible (i.e. U-Pb, zircon fission-track, etc.). Zircon fission-track

www.manaraa.com

dating (ZFT) has the advantage of not requiring the complete dissolution of the zircon grain during analysis, allowing for combined single-grain analyses using two or more geochronological and/or thermochronological techniques.

Although ZFT dating has proven to be an effective and applicable thermochronometer in many cases, it has also encountered limitations in its conventional methodology. The main limitations surround very old zircons as well as younger grains with high uranium concentrations, where track densities are too high to distinguish without a significant counting bias (Montario & Garver, 2009). The present study employs an emerging fission track technique, herein referred to as scanning electron microscope high-density fission-track (SEM-HDFT) dating, in order to date older and higher uranium grains that have previously been unable to be dated by conventional methods. This article aims to apply this new technique in ZFT analysis towards understanding the tectonic and basin evolution of detrital samples in northern Morocco.

Zircon fission-track dating is centered on the accumulation of damage trails formed in the crystal lattice as a result of naturally occurring spontaneous fission of ^{238}U (Tagami & O'Sullivan, 2005). Spontaneous nuclear fission is a process by which heavy, unstable atoms split into sub-equal fragments, releasing neutrons and energy. The positively charged fission fragments are propelled in opposite directions from the site of fission, which if occurring within a dielectric solid leaves behind a damage trail in the crystal lattice. These damage trails, which are referred to as "fission tracks" (Fig. 1), serve as an unconventional daughter product in the uranium isotope decay chain.

www.manaraa.com

Fission-track ages are determined by identifying the density of accumulated tracks in relation to the uranium content of each zircon grain (Price & Walker, 1963; Tagami & O'Sullivan, 2005). The ages determined using this technique differ from the crystallization ages that U/Pb dating provides in that they record the time elapsed since the specific grain was last heated to a certain temperature window, and as such are referred to as cooling ages. Thus, ZFT analysis has become an integral technique in analyzing clastic sediment provenance and exhumation history, both of which are useful in understanding the nature and evolution of sedimentary basins (Bernet & Garver, 2005).

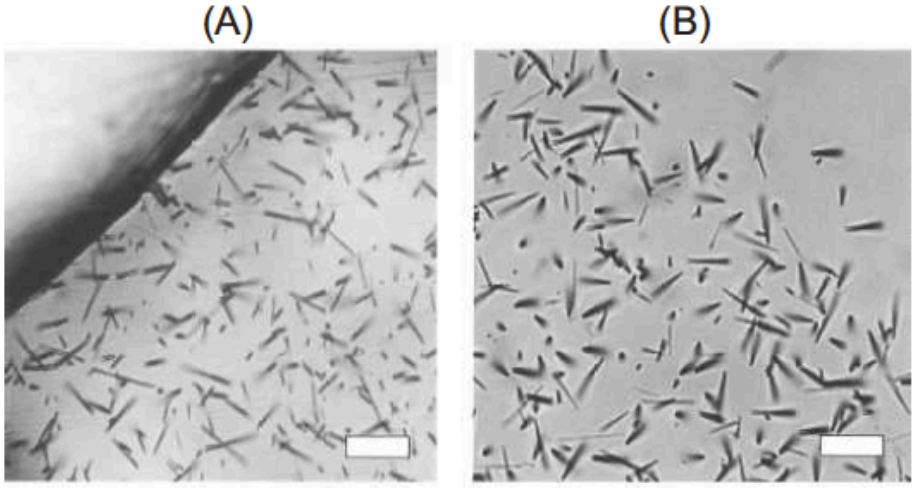

Figure 1.1 Optical photomicrographs of chemically etched fission-tracks:(A) Spontaneous fission-tracks on a polished zircon grain. (B) Neutron irradiation-induced fission-tracks in muscovite detector, providing a mirror image of the spontaneous tracks in grain (Tagami & O'Sullivan, 2005).

Zircon fission-track cooling ages record the time since the grain last passed through an elevated temperature window, although the exact temperature limits for this window vary. The effective closure temperature (T_c) for the ZFT system, that is the temperature above which tracks will be annealed and below which tracks will be retained,

www.manaraa.com

is controlled by the cooling rate. Field-based studies have determined the T_c for zircon to range from ~205-260°C, while laboratory studies yield values ~50-100°C higher (see discussion and references in Montario & Garver, 2009). A simplified and perhaps more appropriate way to define the temperature window for ZFT analyses is the concept of a partial annealing zone (PAZ), which is the range over which fission tracks are partially healed yet still preserved over geologic time scales (Wagner, 1972; Wagner & van den Haute, 1992). Thermal annealing of fission tracks is a process by which the crystal lattice, which becomes disordered by spontaneous fission and α-decay, is gradually restored to an ordered crystalline matrix (Paul & Fitzgerald, 1992; Paul, 1993).

The PAZ represents the depths at which temperatures are elevated enough to partly anneal fission tracks, and is defined as the range of depths/temperatures where 10-90% of tracks are retained (Brandon et al., 1998). Therefore, tracks that are formed in a crystal residing stratigraphically below the PAZ (typically greater depths where temperature increases) will be annealed (see explanation in Tagami & O'Sullivan, 2005), while tracks formed above the PAZ (typically shallower depths, lower temperature) will be wholly preserved within the crystal (Montario & Garver, 2009). Grains that are buried to PAZ depths will have partially annealed tracks, as indicated by shortened track lengths. Fission tracks occur as near perfect cylinders, approximately 8 nm wide, which taper towards each terminal. Latent tracks, those that are unetched and have not been annealed, have a typical length of ~11 μm, however tracks in the PAZ typically range from ~4-10.5 μm (Tagami & O'Sullivan, 2005). The rate at which annealing occurs depends on a number of variables: crystallographic orientation, chemical composition, radiation damage accumulation, pressure, temperature, and time. It should be noted that

www.manaraa.com

the relationship between depth and temperature can vary in certain geologic systems, such as some magmatic regimes, however for the vast majority of systems, and in the sedimentary systems that pertain to the present study in particular it is safe to assume that temperatures increase with depth.

Within the partial annealing zone, there is further variability in the annealing of fission tracks associated with the level of radiation damage within the grain. Grains with high amounts of damage, from both α-particle emission and fission, anneal readily and are "reset" at lower temperatures in the T_c-spectrum. They are thus referred to as low-retentive zircon (Marsellos & Garver, 2010). However, grains with relatively little damage and primarily intact crystal lattices resist annealing at these temperatures, and are thus referred to as highly retentive zircon. The current bounds for the partial annealing zone for radiation-damaged low-retentive zircons is ~195-250°C for 10% retention and ~150-200°C for 90% retention (Reiners & Brandon, 2006).

Fission tracks within zircon are typically 8-10 nm long and 2-5 nm wide, so use of a chemical etchant (in this case, NaOH-KOH eutectic) is required to enlarge the tracks for counting (Fleisher et al., 1975; Wagner & van den Haute, 1992; Tagami & O'Sullivan, 2005). The enlarged tracks can then be counted using an optical microscope to determine the track density, which when related to the uranium concentration, can be used to determine the fission-track cooling age for that grain.

Tagami & O'Sullivan (2005) provide an explanation and derivation of the age calculation equation. The equation has the same principles of other radiometric ages in that it has three parameters: the number of parent nuclides (concentration of ^{238}U), the

www.manaraa.com

number of daughter nuclides (spontaneous fission tracks per unit volume), and the decay constant for the parent nuclides (λ_F). The equation to determine FT age, t, is given by:

$$t = \frac{1}{\lambda_D} \ln\left\{1 + \lambda_D \zeta \rho_D \left(\frac{\rho_S}{\rho_I}\right) QG\right\}$$

such that λ_D is the rate of decay of ^{238}U via α-emission (1.55125×10^{-10} y^{-1}); ρ_D is the induced track density a uranium coated standard glass; ρ_S and ρ_I are the surface density of etched spontaneous and induced fission tracks, respectively; Q is the integrated factor of registration and observation efficiency of fission tracks; and G is the integrated geometry factor of the etched surface. ζ refers to a zeta age calibration that is widely used to determine λ_F (for complete derivation, see discussion in Tagami & O'Sullivan, 2005).

Traditional fission-track dating uses optical microscopes to determine track densities, which limits magnification to ~1500x. Therefore, the upper limit of track densities that can be confidently counted is about 2 x 10^7 tracks/cm^2 (Montario & Garver, 2009). Track densities above this limit become over-etched and indistinguishable by optical techniques, creating a potential bias that does not account for very old, nearly metamict grains, as well as young grains with very high uranium concentrations. To reduce this bias and expose the cooling histories of nearly metamict zircon grains a new method is being developed, utilizing the increased magnification capabilities of scanning electron microscopy.

Scanning electron microscope high-density fission-track dating is an emerging technique that combines a special etching technique and higher magnifications to determine high track densities that would have otherwise been over-etched and useless by

www.manaraa.com

standard optical fission-track methods. Scanning electron microscope high-density fission-track dating requires a retarding etching process, which strategically under-etches the tracks such that they are discernible at magnifications of 3,000-10,000x. This new approach to fission-track dating has recently been employed in understanding thermal evolution accompanying the Grenville orogenic cycle through analyzing Cambro-Ordovician quartzarenites of the Potsdam and Galway Formations of Upstate New York (Fig. 1.2; Montario & Garver, 2009). Grains with track densities up to 3 x 10^8 tracks/cm^2 can be counted using this method, which is about an order of magnitude greater than achievable by standard optical means (Fig. 1.3). The use of scanning electron microscope high-density fission-track analysis has revealed cooling ages in excess of 1.2 Ga, with one grain over 2 billion years old, providing the oldest detrital zircon fission-track ages reported in the literature (Bernet & Garver, 2005; Montario & Garver, 2009).

The present study will employ the use of scanning electron microscopy in analyzing the tectonothermal history of North Africa. Samples taken from the Taza-Guercif basin in northern Morocco, as well as samples from two proximal potential source areas, have been analyzed using detrital ZFT dating to determine cooling history as well as thermal signatures to identify the source area of the sediments. Conventional, optically based fission-track methodologies are ill-suited for determining track densities for the zircon grains found in these samples as they demonstrate a high degree of radiation damage, which in turn makes determining track densities difficult at lower magnifications (~1,200x for optical microscopy vs. up to 10,000x using SEM). The findings will then be interpreted within the context of both recent and ancient North African geology, as well as future applications for the new fission-track technique.

www.manaraa.com

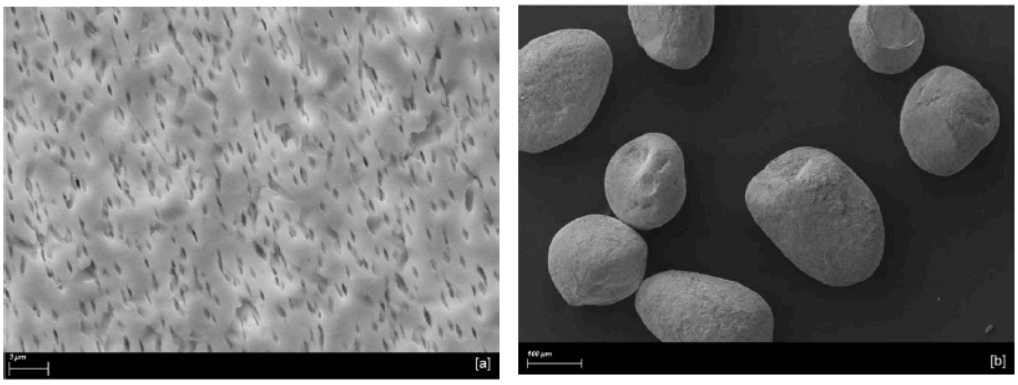

Figure 1.2 (A) SEM image of etched fission-tracks in zircon from the Potsdam Formation, which has a track density that is too high to count optically. (B) SEM image of well-rounded, pitted, high radiation damaged zircon from the Potsdam Formation (Image from Montario & Garver, 2009).

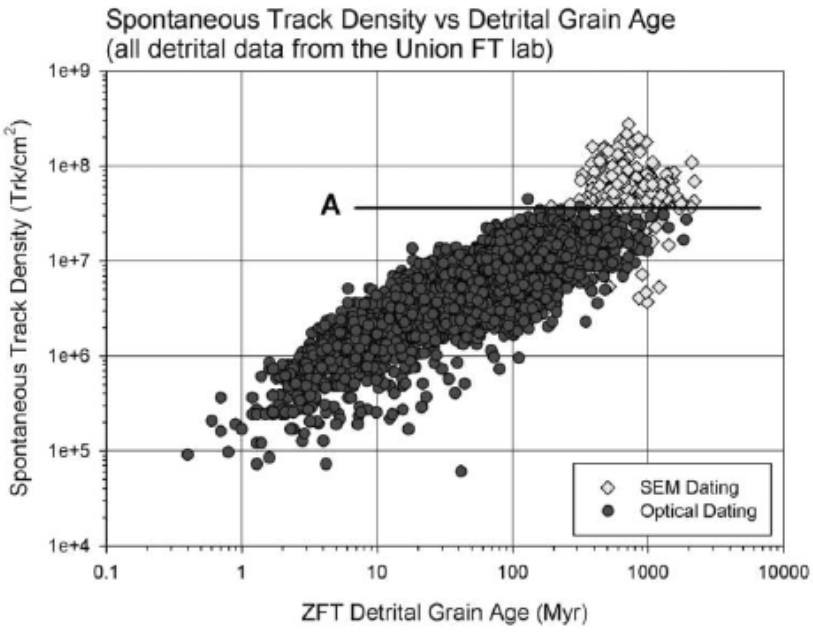

Figure 1.3 Spontaneous track density versus detrital grain age from various studies in the Union College fission-track (FT) lab. Circles denote grains dated by standard optical FT at 1250x; diamonds denote grains dated using the new SEM-HDFT dating technique. SEM-HDFT has allowed for determination of track densities approximately one order of magnitude above the upper limits of optical FT dating, denoted by the line marked "A" (Image from Montario & Garver, 2009).

www.manaraa.com

1.1 GEOLOGIC BACKGROUND

Modern-day Africa is an amalgamation of five major Archean cratons (West Africa, Congo, Tanzania, Kaapvaal, and Kalahari), as well as several large continental blocks (Rino et al., 2008). The tectonothermal events that closed large Proterozoic ocean basins (Mozambique, Adamastor, Damara, and Trans-Sahara) leading to the collision of Archean cratons, and eventual suturing of those cratons with mobile collisional belts are collectively known as the Pan-African orogenic cycle (Kröner & Stern, 2005; Rino et al., 2008). The Pan-African spanned a period of ~870 to ~550 Ma, culminating in the formation of the Neoproterozoic supercontinent Gondwana (Kröner & Stern, 2005). Together with the Grenville orogeny (1.2-1.0 Ga), the Neoproterozoic is regarded as the most active period in Earth's history in terms of crustal formation (Kröner & Stern, 2005; Rino et al., 2008).

Morocco, situated in the northwesternmost corner of Africa, consists of a number of topographic features resulting from several orogenic events and Cenozoic interactions between Africa and Eurasia (Gomez et al., 2000). These features include the Moroccan Atlas Mountains, several plateaux (mesetas), and the Betic-Rif-Tell mountains (Fig. 1.4). The Moroccan Atlas are further divided into the High Atlas, Middle Atlas, and Anti-Atlas, which collectively comprise a system of inverted-failed rift basins derived from the opening of the Neo-Tethys and Atlantic oceans in the Mesozoic (Gomez et al., 2000). The Middle Atlas and High Atlas, which continue into Algeria as the Saharan Atlas, are 100-km wide intracontinental fold-thrust belts in the foreland of the Betic-Rif-Tell orogen, each reaching altitudes of 2000 meters or more (Babault et al., 2008). The Anti-Atlas Mountains, which lie further to the south, represent an up-warped extensive massif

www.manaraa.com

that exposes a Hercynian fold belt with limited influence from Alpine activity (Gomez et al., 2000; Babault et al., 2008). North of the High Atlas, are the Moroccan Meseta and High Plateau, which are separated to the west and east by the Middle Atlas, respectively. These two large crustal blocks sit on average ~1200 meters above sea level and underwent very little Cenozoic deformation, with the Middle Atlas accommodating the majority of shear strain during that time (Gomez et al., 2000; Babault et al., 2008; Barbero et al., 2011).

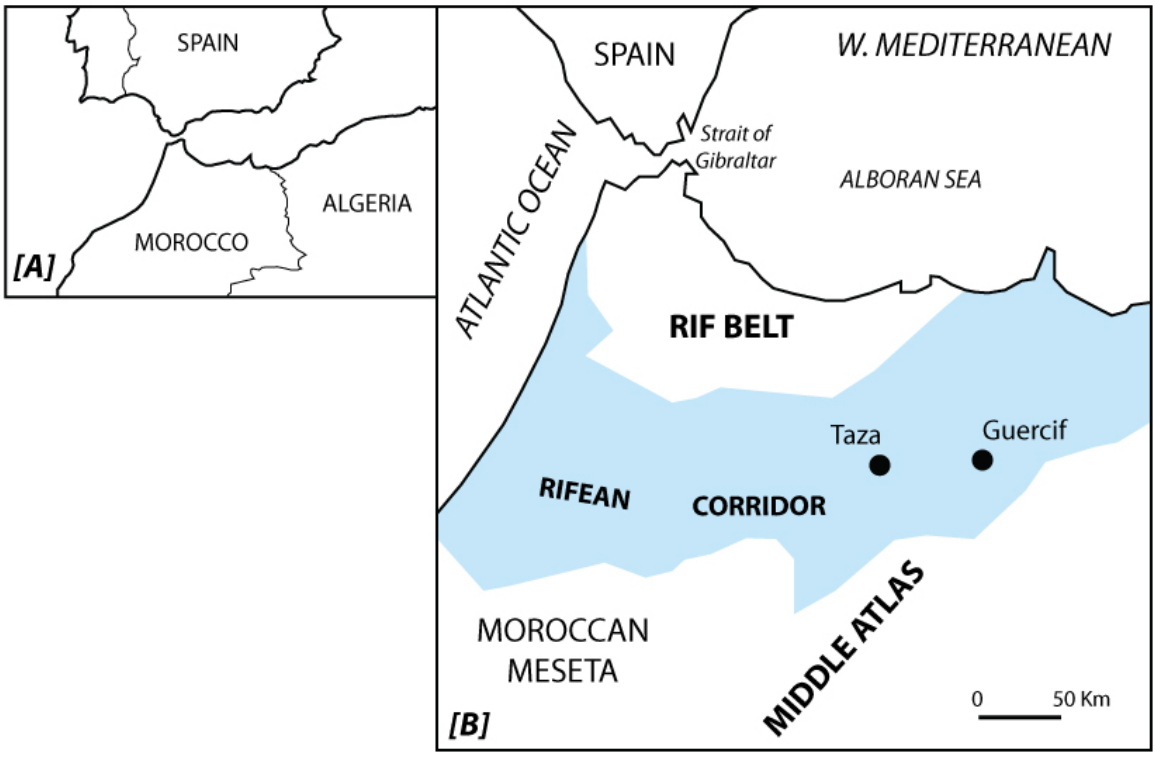

Figure 1.4 [A] Geography of North Africa; [B] Detail showing the Taza-Guercif basin with respect to the Rifean Corridor, Rif Belt, and Middle Atlas mountains in northern Morocco.

The northernmost part of Morocco, along the Mediterranean coasts of Africa and Iberia, consists of the Betic-Rif-Tell Alpine mountain chains. The Moroccan Rif, Algerian Tell, and Iberian Betic mountains are each further divided into allochthonous

www.manaraa.com

internal and autochthonous external zones, which form an arcuate chain that surrounds the Alboran Sea (Gomez et al., 2000).

In order to understand the tectonic evolution of northwestern Africa, particularly with respect to its role in the Messinian salinity crisis, this study examines the cooling history of detrital zircon grains from the Taza-Guercif basin of northern Morocco (see Figs. 1.4 & 1.5). The Taza-Guercif basin lies along the southern margin of the Rifean Corridor, a paleomarine passageway between the Middle Atlas and the Rif that linked the Atlantic Ocean to the Mediterranean during the Miocene (see Fig. 1.4). The Rifean Corridor constitutes the foreland basin of the Betic-Rif orogen, which has since in-filled with Neogene-Quaternary sediments, forming numerous sub-basins. During Miocene times, the Rifean Corridor contributed to the Messinian salinity crisis, which is widely considered to be among the most extensive evaporitic events in Earth's history, as well as one of the most dramatic changes in sea level in the last 20 Myr (Krijgsman et al., 1999; Rouchy & Caruso, 2006). Beginning with an assumedly synchronous onset at 5.96 Ma and ending with the Zanclean Flood at 5.33 Ma, the Messinian salinity crisis led to the almost complete desiccation of the Mediterranean Sea, the deposition of up to 3500 m of evaporates in the eastern Mediterranean, sequestration of 6% of global ocean salinity, and extensive subaerial erosion of the margins of the basin (Hsü et al., 1977; Krijgsman et al., 1999a; Krijgsman et al., 1999b; Rouchy & Caruso, 2006). It is widely acknowledged that both glacio-eustatic changes and tectonics influenced the onset of the Messinian salinity crisis, however the two strongest glacial stages post-date the onset of evaporite deposition by ~200 Kyr, suggesting that local tectonics likely played a significant role (Rouchy & Caruso, 2006).

www.manaraa.com

The Taza-Guercif basin includes a ~1500m marine and continental stratigraphic succession (Figs. 1.5 & 1.6; Gelati et al., 2000; Krijgsman et al., 1999a). The filling of the Rifean foredeep is largely considered to have progressively restricted and completely isolated the Mediterranean from the global ocean during the Messinian Salinity Crisis, though the timing of which is poorly constrained (Krijgsman et al., 1999a). The Messinian Salinity Crisis is particularly of interest considering its large scale, short duration, local sea level change upwards of a kilometer, erosion of exposed seafloor, as well as affecting global ocean circulation and eustatic sea level change (Rouchy & Caruso, 2006).

www.manaraa.com

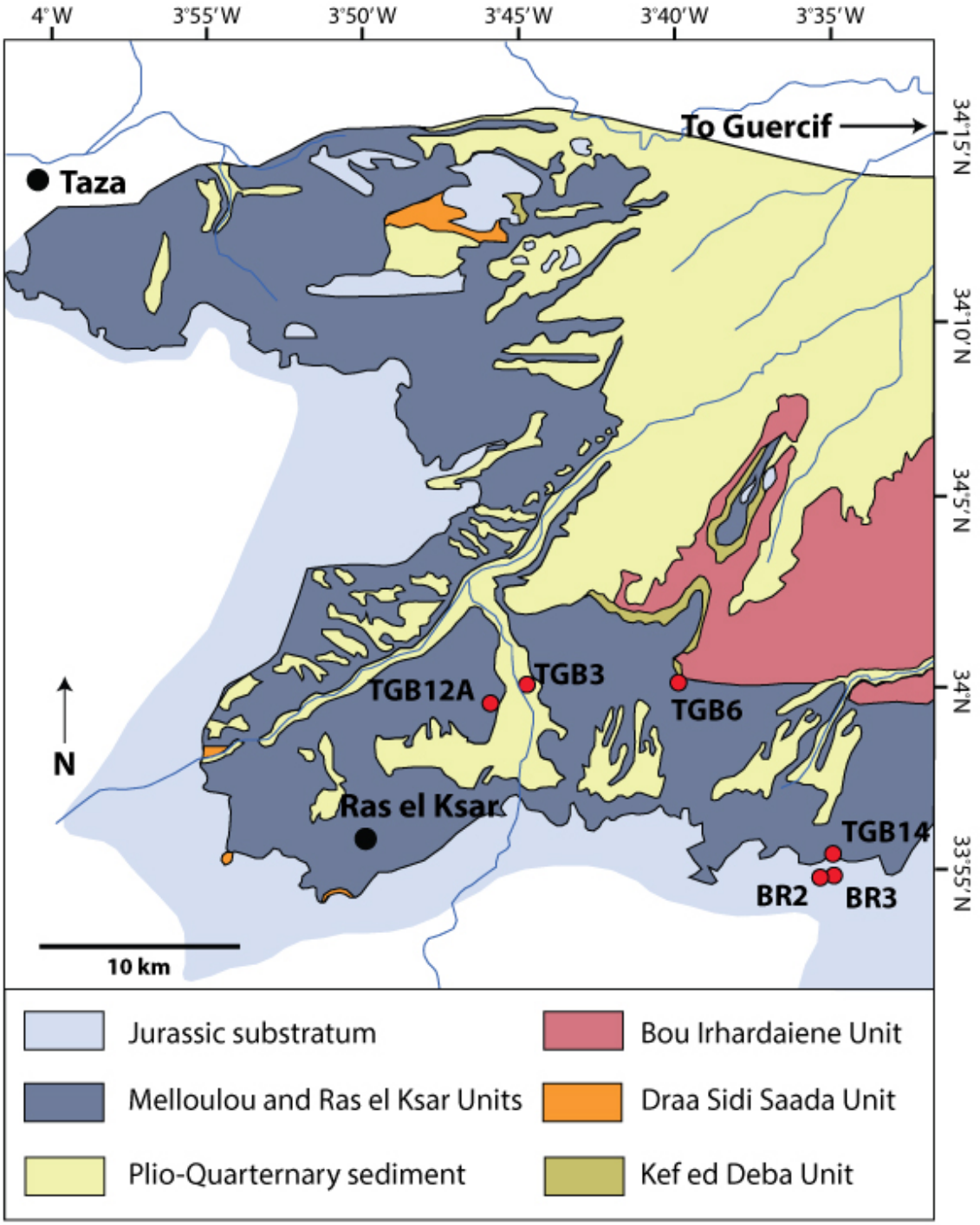

Figure 1.5 Location of samples collected from the Taza-Guercif basin, which lies along the southern margin of the Rifean Corridor in northern Morocco.

www.manaraa.com

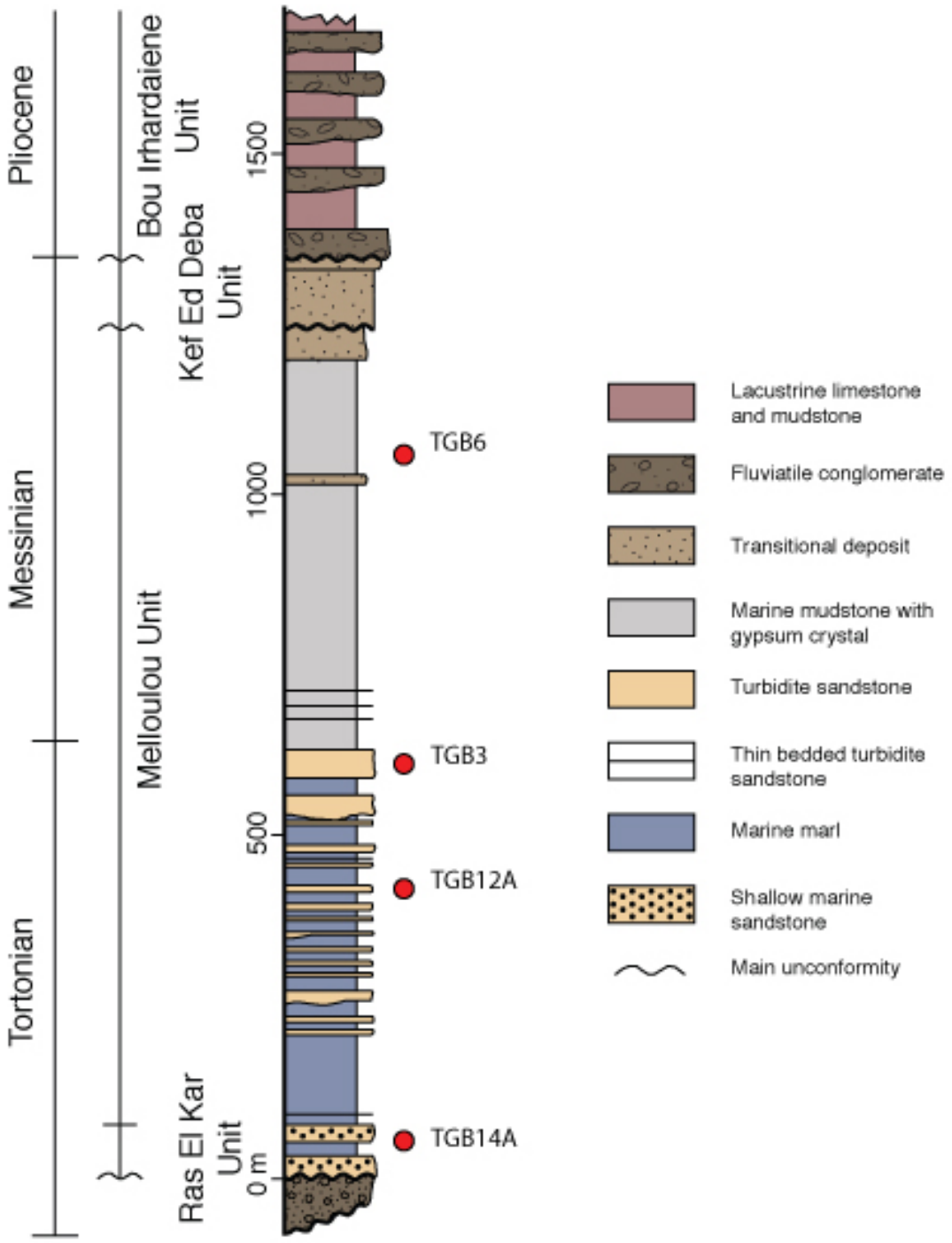

Figure 1.6 Stratigraphic section showing the location of samples collected from the Taza-Guercif basin for SEM-HDFT analysis.

www.manaraa.com

The purpose of the present study is to further development of the SEM-HDFT technique and to explore its applicability in evaluating the source-to-sink system of the Taza-Guercif basin in the context of the Messinian salinity crisis. Zircons were extracted from four samples from the Taza-Guercif basin of northern Morocco, as well as five samples taken from two of the most proximal and probable sources (Rif, 3; Middle Atlas, 2). The zircons collected show signs of metamictization, a process by which the crystal lattice has degraded over time due to radiation damage (α-decay and spontaneous fission) and will eventually become amorphous. Zircons in this state are most susceptible to thermal annealing, and as such should yield information regarding heating to the lowest levels of the partial annealing zone. While it is evident that sediments in the basin have not been buried to depths necessary to thermally reset fission tracks in zircon (approximately 8 km, assuming a normal geothermal gradient), determining cooling ages for the basin sediments, as well as from the two proximal and therefore most probable sources (Rif and Middle Atlas), could provide valuable information not only about the source of sediments for the Neogene-Quaternary basin but also in understanding the long-term thermal history of North African-Eurasian convergence.

www.manaraa.com

CHAPTER 2

SAMPLES & METHODS

2.1 SAMPLE DESCRIPTIONS

Whole rock samples were collected from the following zircon-bearing units in the Taza-Guercif basin (Figs. 1.5 & 1.6), as well as from its two probable source areas. Basin sandstone samples were collected from the El Rhirane (T1) and Tachrift (T2) Turbidite Formations, Kef Ed Deba Formation, Ras el Ksar Formation, and Gypsiferous Marl Formation. Samples from the two possible source areas were collected from the Ketama and Tisirene Units of the Rif Mountains, as well as Jurassic substratum of the Middle Atlas (Bou Rached). Depositional ages and locations of samples are provided in Table 2.1.

The Ras el Ksar Formation is a heterogenous succession of shallow marine sediments that shows a significant variability of facies and thickness from marginal marine to outer shelf depositional facies (Gelati et al., 2000). The Ras el Ksar is characterized by cross-laminated sandstone beds alternating with thin-bedded rippled sandstones. The Tachrift T2 Turbidites consist of several turbidite systems separated by similar thicknesses of mudstone. The T2 Turbidites total ~600 meters in vertical thickness and are several hundred meters in lateral extent, with a sand:mud ratio that exceeds 10 in some locations (Gelati et al., 2000). In contrast, the El Rhirane Turbidites are thinly bedded with sand-mud ratios <<1 (Bernini et al., 1994). The Gypsiferous Marls

www.manaraa.com

constitute the upper part of the Melloulou Unit and consist of more than 600 meters of yellowish and grayish blue marls that are erosionally truncated at the top (Bernini et al., 1994; Gelati et al., 2000).

The two likely sources for the aforementioned detrital units are the Rif and Middle Atlas ranges. The Ketama and Tisirene units of the Rif consist of intensely folded, low grade-metamorphosed marls and limestones and flysch nappes, respectively (Chalouan et al., 2001; Chalouan et al., 2008). The Jurassic substratum of the Bou Rached sandstone formation of the Middle Atlas locally consists of 10-50 cm thick planar beds of fine-grained sandstones.

Table 2.1 Taza-Guercif basin and source sample names, ages, and locations

Sample Name	Formation/Unit	Depositional Age	Latitude	Longitude
Basin Samples				
TGB3	Tachrift T2 Turbidites	Tortonian-Messinian	33°59'53.42"N	3°44'21.78"W
TGB6	Gypsiferous Marl	Tortonian-Messinian	34°0'6.13"N	3°39'32.49"W
TGB12A	El Rhirane T1 Turbidites	Tortonian-Messinian	33°59'39.77"N	3°45'43.28"W
TGB14A	Ras el Ksar	Tortonian	33°55'20.65"N	3°34'34.23"W
Probable Sources				
RF2	Ketama (Rif)	Liassic-Late Cretaceous	34°58'23.78"N	3°48'56.10"W
RF3	Ketama (Rif)	Liassic-Late Cretaceous	35°1'31.84"N	3°49'19.95"W
RF4	Tisirene(Rif)	Liassic-Late Cretaceous	35°6'24.65"N	4°0'6.96"W
BR2A	Bou Rached (Middle Atlas)	Jurassic	33°54'48.45"N	3°34'49.26"W
BR3	Bou Rached (Middle Atlas)	Jurassic	33°54'47.99"N	3°34'45.88"W

2.2 LABORATORY METHODS

Zircon was separated from the whole rock samples by conventional methods. Whole rock samples were crushed and pulverized before density separation using a

www.manaraa.com

Gemeni® shaker table, a Frantz® magnetic separator, and finally through a two-stage heavy liquid separation process using a solution of lithium heteropolytungstates in water (LST) and methylene iodide.

Following separation and optical inspection of zircon, grain mounts were made for each sample by embedding several hundred grains in ~2 x 2 cm^2 PFA Teflon® (tetrafluoroethylene-perfluoroalkoxyethene) squares. Such an abundance of grains per mount is necessary as a large portion will be uncountable due to heterogeneous uranium distribution, completely metamictized by radiation damage, removed or over-polishing in the polishing process, as well as many other factors that are typical of detrital zircon grains (Bernet & Garver, 2005). Three Teflon® mounts were made for each sample as well as three natural age standards: the Buluk Tuff (16.4 ± 0.2 Ma), Fish Canyon Tuff (27.9 ± 0.5 Ma), and Peach Springs Tuff (18.5 ± 0.1 Ma)(Garver, 2002). The zircon-embedded Teflon® mounts were then polished on a Buehler AutoMet® 2000 Powerhead and EcoMet® 3000 Variable Speed Grinder/Polisher; first using a 9 μm diamond slurry, and then again with a 1 μm diamond slurry. The first round of polishing exposes the zircon grains, which were previously embedded in the Teflon®. The first round of polishing (9 μm) was done at 420 rpm for 10 minutes at 18 pounds of pressure. The second round of polishing (1 μm) was done at 420 rpm for 8 minutes at 15 pounds of pressure to remove polishing scratches from exposed zircon grains, leaving a liquid-clear finish. For each round of polishing, the pressure was distributed over three sample mounts and three blanks for even polishing.

The finely polished and mounted zircon grains were then inspected at 500x magnification to assure the clarity and quality of the polishing. After polishing, the

www.manaraa.com

mounts were etched in a KOH:NaOH eutectic at 228°C. While typical optical fission-track analyses require extensive etching to enlarge tracks for counting, SEM-HDFT analyses require significantly less etching. The samples therefore were etched for 5-7 hours. The strong base solution etches the fission tracks that have occurred naturally in the zircons due to spontaneous radioactive decay. Typically, etch times are much longer (~15-30 hours) in order to etch tracks for analysis using optical microscopy, however because of the enhanced magnification power of scanning electron microscopy, tracks that would be considered "under-etched" by optical means may be counted and higher track densities may be discerned (Garver, 2003). The ideal etch time differs from sample to sample in that younger grains require longer etch time than older grains, which have a higher degrees of radiation damage (see Bernet and Garver, 2005). Once removed from the etchant, the mounts were pressed between two glass plates for 20 minutes at 228°C and then allowed to cool to room temperature. After flattening, the mounts were sonicated in 100 ml of 6N hydrochloric acid (20%) for 10 minutes. The mounts were then rinsed in distilled water, and then again in ethanol, and then left to dry on a hot plate (75° C for 5 minutes). The cleaned and flattened mounts were then affixed with a low-uranium, pre-annealed, freshly cleaved flake of mica with a thickness of about 0.2 mm. Three Corning CN-5 glass dosimeters, which have a known ^{238}U content of 11 ppm, were also affixed with freshly cleaved flakes of mica.

The mica-affixed mounts and glass dosimeters were sent to Oregon State University's TRIGA Mark II Research Reactor (OSTR) for irradiation. The mounts were arranged in a stack, taped, and then placed in a polyethylene tube with a glass dosimeter at the top, bottom, and middle of the stack to determine the fluence applied to

www.manaraa.com

each position in the stack during irradiation. The order of the glass dosimeters and zircon mounts was clearly documented, and the mass of the polyethylene tube, the stack of mounts, and the Styrofoam used for packing were determined for calculation of radionuclides expected after irradiation. During irradiation, the samples received a nominal fluence of 2 x 10^{15} neutrons/cm^2.

Following irradiation, samples were isolated for several weeks while radioactive isotopes with shorter half-lives decayed. The stack of glass dosimeters, Teflon® mounts, and mica detectors were then separated and the mounts and detectors were pierced using a carbide-tipped scribe to create registration points. These registration points are used to align the mounts and detectors for the counting process. The mica detectors were then etched in 48% hydrofluoric acid for ~18 minutes at room temperature (20-22° C). The mica was then cleaned using NaOH and water, then ethanol, and finally left to dry on a hot plate at ~100° C. The Teflon® mounts and their corresponding mica detectors were mounted as mirror images on a petrographic slide using thin section epoxy and a glass cover slip to account for the difference in height.

A layer of carbon ~80-100 Å (8-10 nm) thick was then applied to the slides using a sputter-coater to prevent charging. The grains and micas were then imaged at ~3,000-10,000x using a Zeiss® EVO50 tungsten-filament scanning electron microscope. The range of magnifications was due to variations in grain surface quality and track clarity, however each grain-mica pair was imaged using the same magnification. The images were taken using a secondary electron detector, which progressively scans the surface, collecting electrons released by the sample. A very slow, line-integrated scan speed was used (~6 min/image), as it provided the highest resolution image for counting purposes.

www.manaraa.com

The secondary electron images of the grain-mica pairs were then analyzed using ImageJ, which is a public domain, Java-based image-processing program developed by the National Institutes of Health. Using this software, the counting area can be measured and the fission tracks may be counted in order to determine the spontaneous and induced track densities for the grain and mica, respectively. The number of spontaneous tracks in the zircon, the number of induced tracks in the mica, and the area of the image used for counting were then entered into the ZetaAge and BinomFit (Brandon, 1996) software to determine individual grain ages and peak-fit age populations (see APPENDIX C).

www.manaraa.com

CHAPTER 3

RESULTS

Nine total samples were analyzed using the new scanning electron microscopy high-density fission-track dating technique. Four of these samples were taken from the Taza-Guercif basin itself, while the remaining five samples represent the two most proximal and probable sources: the Rif mountains (3) and the Middle Atlas (2). Probability density plots with component peak ages for each individual sample, as well as summary plots for each unit (Taza-Guercif basin, Rif, and Middle Atlas) can be seen in Figures 3.1, 3.2, and 3.3.

Upon a preliminary assessment of all of the samples, each returned Mesozoic and older cooling age populations, suggesting that the zircons had not been thermally annealed, or reset, following recent burial or tectonic activity. As no clear distinction could be made between the basin sediments versus either of the two probable source areas, a larger population of grains was imaged from two of the basin samples (TGB12A, TGB14B; approximately 40 grains each) in order to get a higher resolution cooling history for the area. A summary of fission track parameters and grain age population information for all samples can be found in Tables 3.1 and 3.2, respectively (see APPENDIX C for complete data).

In each of the samples analyzed, the majority age population (P1) is >300 Ma. Samples in general returned two component peak ages, though some younger (100-200

www.manaraa.com

Ma), minor age peaks are noted, each accounting for no more than about 25% of grains for each sample. The Taza-Guercif basin samples returned single grain ages of 117.3-1202.0 Ma. When the Taza-Guercif basin samples are grouped and analyzed as a single detrital sample, P1 is 323.8 ± 20.8 Ma (49.2%) and P2 is 612.3 ± 39.7 Ma (33.9%). The Rif samples, which range in single grain ages from 71.8-1575.9 Ma, when grouped return a P1 age of 433.4 ± 22.5 Ma (88.7%) and a P2 age of 114.6 ± 11.6 Ma (11.3%). The grouped Middle Atlas samples, though having a smaller range of single grain ages (126.1-878.3 Ma) are quite similar to the Rif when grouped, with a P1 age of 435.8 ± 29.2 Ma (72.9%) and a P2 age of 160.0 ± 15.7 Ma (27.1%).

While there were some noticeable distinctions between each of the samples, when analyzed all together two very distinct age populations were identified, combining for ~85% of the grains: a P1 age of 319.1 ± 16.7 Ma (50.8%), and a P2 age of 607.2 ± 34.7 Ma (35.8%). The cooling age populations suggest a relatively long period of thermal stability in northern Morocco, with temperatures and burial depths insufficient to thermally anneal zircon fission tracks (~240 °C).

www.manaraa.com

Table 3.1 Zircon fission track data; Taza-Guercif Basin, Rif, and Middle Atlas samples

Sample	ρ_s	N_s	ρ_i	N_i	ρ_d	N_d	n	χ^2	Age	-1σ	+1σ	U ± 2se
Taza-Guercif Basin												
TGB3A	5.51×10^7	6994	7.12×10^6	904	3.307×10^5	3008	40	0.0	399.0	-19.1	+20.1	265.0 ± 19
TGB6B	3.62×10^7	1820	6.15×10^6	309	3.434×10^5	3008	11	0.0	317.2	-21.5	+23.1	220.3 ± 26
TGB12A	5.14×10^7	5570	8.14×10^6	881	3.345×10^5	3008	35	0.0	331.5	-16.2	+17.1	299.2 ± 22
TGB14B	5.43×10^7	2393	7.85×10^6	346	3.396×10^5	3008	13	0.0	366.9	-23.6	+25.2	284.4 ± 32
Rif												
RF2A	6.10×10^7	2480	7.96×10^6	324	3.128×10^5	3009	12	0.0	373.2	-24.2	+25.8	313.2 ± 38
RF3A	3.76×10^7	2016	6.21×10^6	333	3.089×10^5	3009	12	0.0	293.8	-19.1	+20.5	247.2 ± 28
RF4A	6.33×10^7	2188	6.16×10^6	213	3.051×10^5	3009	11	0.0	484.7	-36.0	+38.7	248.3 ± 35
Middle Atlas												
BR2A	4.31×10^7	2093	5.26×10^6	255	3.141×10^5	3009	15	0.0	401.5	-28.2	+30.3	205.8 ± 26
BR3C	3.55×10^7	1539	6.60×10^6	286	3.153×10^5	3009	11	0.0	267.1	-18.6	+19.9	257.5 ± 31

Note: In this table, Age is the pooled age; ρ_s is the density (cm^2) of spontaneous tracks and N_s is the number of spontaneous tracks counted; ρ_i is the density (cm^2) of induced tracks and N_i is the number of induced tracks counted; ρ_d is the density (cm^2) of tracks on the fluence monitor (CN5) and N_d is the number of tracks on the monitor; n is the number of grains counted; χ^2 is the Chi-squared probability (%). Zircon fission track ages (± 1σ) were determined using the Zeta method, and calculated using the computer program and equations in Brandon (1992). A Zeta factor of 321.9 ± 10.6 (± 1 SE) is based on 7 determinations on standard samples from the Fish Canyon Tuff and Buluk Tuff. Glass monitors (CN5) placed at the top and bottom of the irradiation package were used to determine the fluence gradient. All samples were counted on a Zeiss EVO50 scanning electron microscope at magnifications ranging from 4,000-10,000x.

www.manaraa.com

Table 3.2 Binomial component ages of detrital zircon fission-track data: Taza-Guercif Basin, Rif, and Middle Atlas samples

Sample	Etch Time (hrs)	n	Age range (Ma)	P1	P2	P3	P4
Taza-Guercif Basin							
TGB3A	5	40	124.5-994.4	591.1 ± 45.9 52.4%	322.1 ± 34.6 34.2%	172.4 ± 18.5 13.4%	
TGB6B	5	11	117.4-923.1	371.2 ± 31.0 74.5%	175.3 ± 26.5 25.5%		
TGB12A	5	35	162.9-1204.5	313.2 ± 26.1 64.7%	610.9 ± 72.5 22.8%	203.2 ± 34.5 12.5%	
TGB14B	5	13	184.8-1035.7	569.2 ± 57.6 52.4%	231.2 ± 22.2 47.6%		
All TGB		99	117.3-1202.0	323.8 ± 20.8 49.2%	612.3 ± 39.7 33.9%	191.7 ± 15.4 16.9%	
Rif							
RF2A	7	12	116.7-722.8	424.5 ± 30.2 91.7%	117.3 ± 19.5 8.3%		
RF3A	7	12	71.8-693.6	389.9 ± 31.5 73.7%	114.2 ± 14.2 26.3%		
RF4A	5	11	316.4-1572.7	393.4 ± 50.0 69.2%	940.8 ± 332.2 30.8%		
All Rif		35	71.8-1575.9	433.4 ± 22.5 88.7%	114.6 ± 11.6 11.3%		
Middle Atlas							
BR2A	5	15	159.1-878.3	452.2 ± 36.2 85.5%	174.2 ± 36.6 14.5%		
BR3C	5	11	126.1-722.4	407.6 ± 45.5 56.2%	156.0 ± 17.6 27.1%		
All Middle Atlas		26	126.1-878.3	435.8 ± 29.2 72.9%	160.0 ± 15.7 27.1%		
All Samples		**160**		**319.1 ± 16.7** **50.8%**	**607.2 ± 34.7** **35.8%**	**159.4 ± 10.9** **12.9%**	**75.3 ± 27.6** **0.5%**

Note: n = number of dated grains; Uncertainties are cited at 68% confidence interval (about ±1 SE; asymmetric errors are averaged). Percentages below the age population peaks denote the relative abundance of grains falling within those peaks for that sample. Zircon grains were dated using standard methods for FT dating using an external detector. Zircons were extracted using standard separation procedures. Fission-tracks were counted on Zeiss EVO50 scanning electron microscope. Total magnifications vary between 4,000-10,000. A Zeta factor of 321.9 ± 10.6 (±1 SE) was computed from 7 determinations on standard samples (Fish Canyon Tuff and Buluk Tuff). This table shows all binomial peak fitted ages calculated using Binomfit 1.2.62 (Brandon, 1992).

www.manaraa.com

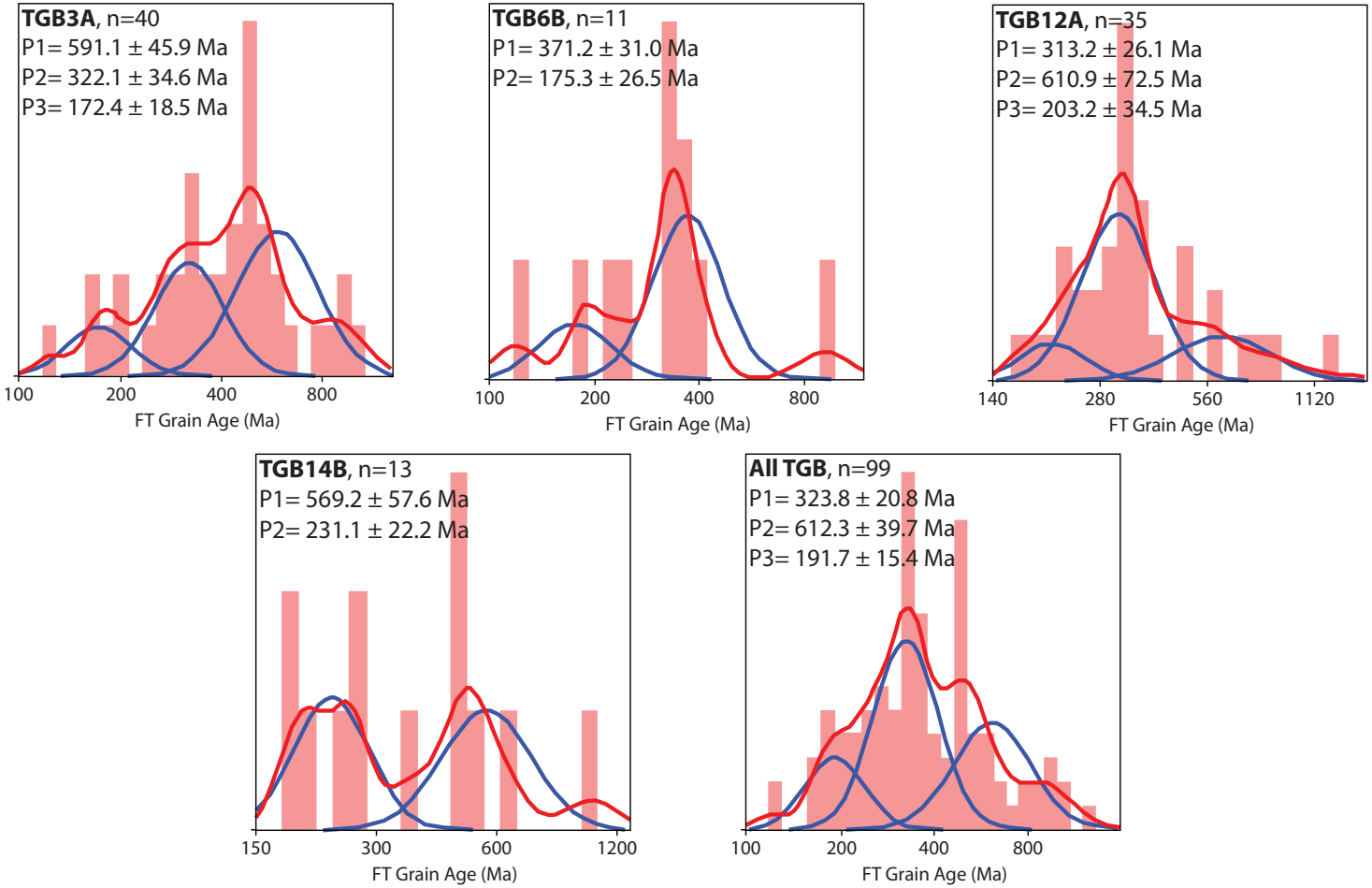

Figure 3.1 Probability density plots of zircon fission track cooling ages for samples collected from the Taza-Guercif basin in northern Morocco. Red curve denotes polynomial age distribution, whereas blue curves represent individual component peaks. P1 represents the majority age population, with subsequent peaks decreasing in abundance.

www.manaraa.com

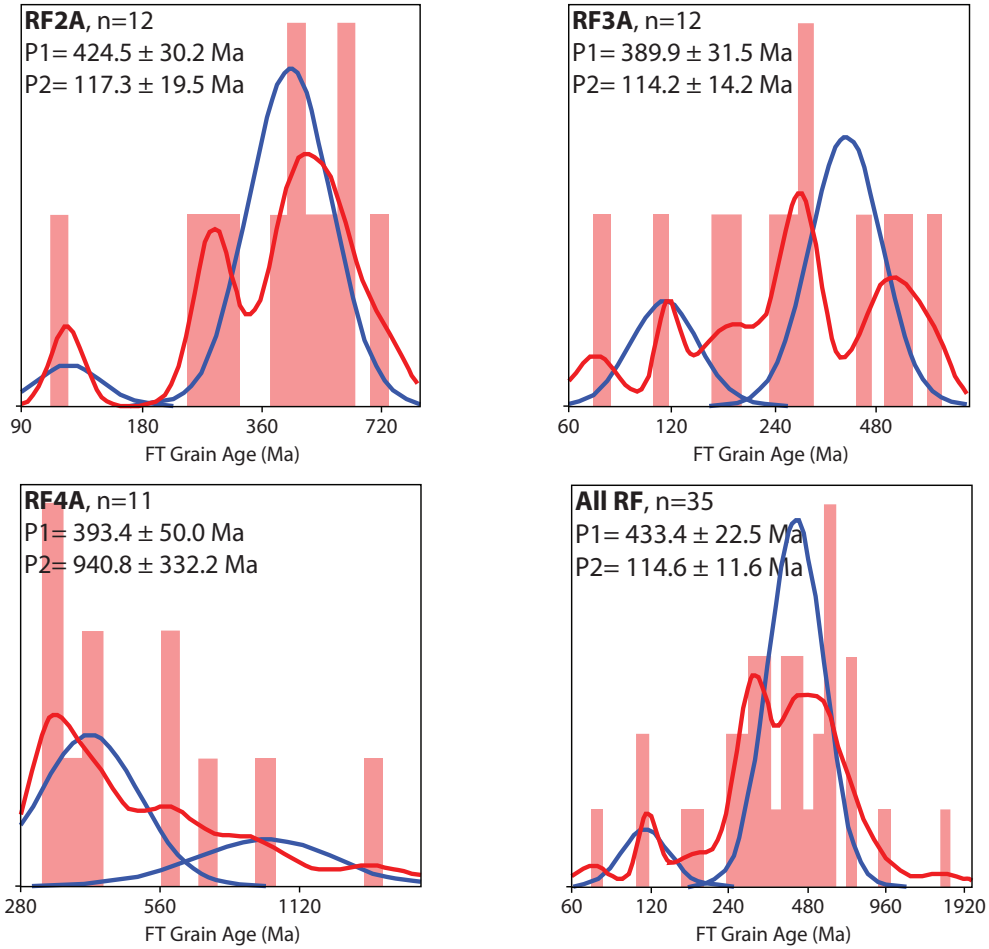

Figure 3.2 Probability density plots of zircon fission track cooling ages for samples collected from the Rif, representing one of the two proximal and probable source areas for Taza-Guercif basin sediments. Red curve denotes polynomial age distribution, whereas blue curves represent individual component peaks. P1 represents the majority age population, with subsequent peaks decreasing in abundance.

www.manaraa.com

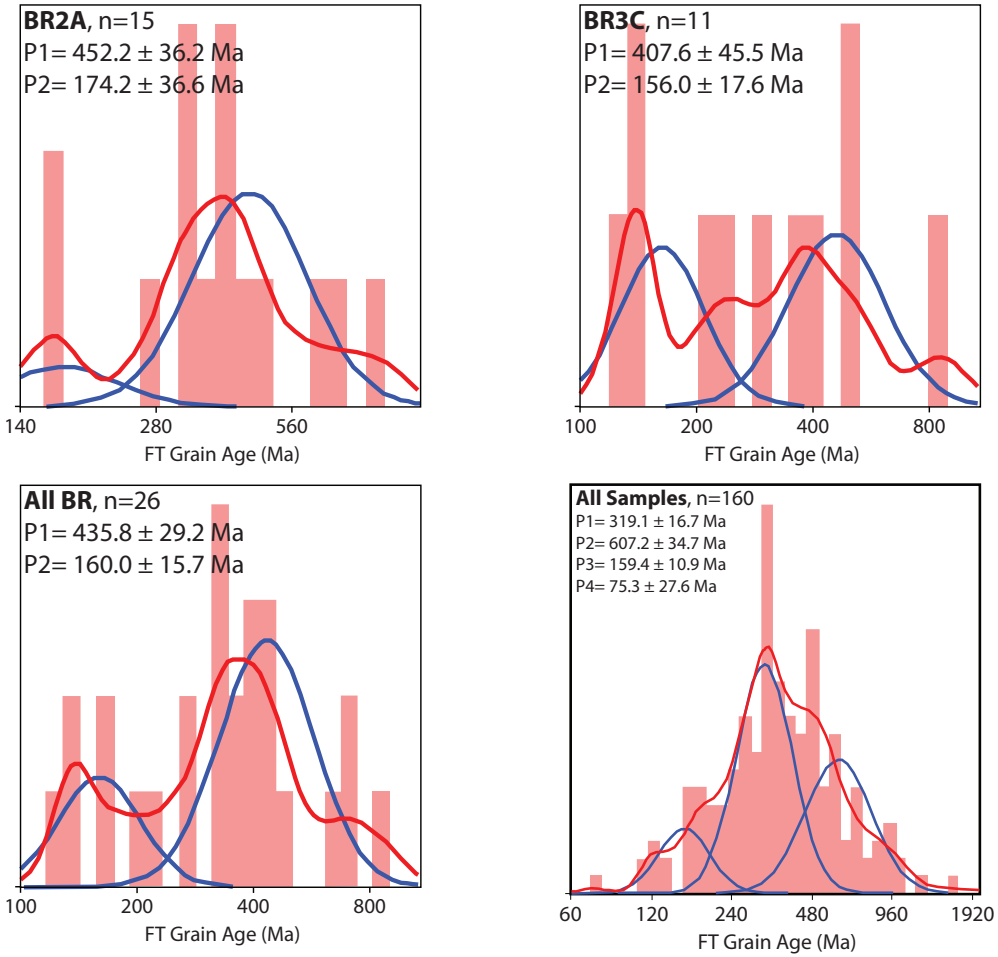

Figure 3.3 Probability density plots of zircon fission track cooling ages for samples collected from the Middle Atlas, representing the second of the two proximal and probable source areas for Taza-Guercif basin sediments. Red curve denotes polynomial age distribution, whereas blue curves represent individual component peaks. P1 represents the majority age population, with subsequent peaks decreasing in abundance.

www.manaraa.com

CHAPTER 4

DISCUSSION & FUTURE APPLICATIONS

4.1 DISCUSSION OF RESULTS

The present study set out to better understand the tectonic and thermal history of North Africa by determining the source and cooling history of sediments in the Taza-Guercif basin of northern Morocco. The majority peak ages for the probable source areas—the Rif and Middle Atlas mountains—are very similar, therefore making it difficult to definitively attribute one versus the other as the dominant source for the basin sediment. The similarities in the cooling ages of the Rif Belt samples and the more southern Middle Atlas samples might suggest that a regional-scale uplift event is responsible. In this scenario, both the Rif and the Middle Atlas appear to have contributed significant sediment supply to the Taza-Guercif basin prior to the Messinian salinity crisis.

While the two sediment source areas have similar P1 ages (433.4 ± 22.5 Ma, 435.8 ± 29.2 Ma), there are slight differences in the P2 ages. The Rif samples collectively show a minority cooling age population at 114.6 ± 11.6 Ma. The Middle Atlas samples, on the other hand, yield a slightly older P2 population at 160.0 ± 15.7 Ma, which approaches being within error of the P3 population of the Taza-Guercif basin samples (191.7 ± 15.4 Ma), which could indicate a stronger contribution of sediment coming from the south from the Middle Atlas. This might suggest that Cenozoic uplift of the Middle

www.manaraa.com

Atlas, though not recorded in the fission-track ages, played a more predominant role in triggering the Messinian salinity crisis, however the relatively small number of Middle Atlas grains analyzed makes such a connection inconclusive.

Although a definitively diagnostic thermal signature could not be established to link the basin sediments to a single, direct source area, the cooling ages revealed using the new scanning electron microscopy high-density fission-track dating technique nonetheless provide useful information regarding the source-to-sink systems associated with African-Eurasian convergence. Through SEM-HDFT dating, significant cooling age populations for detrital zircon of northern Morocco were revealed at 319.7 ± 16.7 Ma and 607.2 ± 34.7 Ma, both of which approach and/or exceed the upper limits of conventional fission-track dating capability due to the densities of tracks that much be differentiated and counted. These two age populations correspond with the Hercynian and Pan-African orogenies, respectively, which is of no surprise as the Pan-African is considered to be among the largest crustal events in Earth's history. Therefore, the Pan-African population (~607 Ma) likely reflects cooling associated with the crystallization of zircon during the formation of Gondwana, rather than the reheating and annealing of pre-existing zircon passing through the partial annealing zone. If this assumption is correct, then SEM-HDFT should be considered an effective and reliable geochronometer. The Hercynian population (~320 Ma), however, could represent the crystallization of new zircon, the heating of previously crystallized zircon, or the exhumation of deeply buried rock during the final stages of the assembly of Pangaea in the Carboniferous.

It must be noted that the present study is by no means a full-spectrum fission-track analysis of the zircon samples, but instead an investigation into the oldest grains

www.manaraa.com

that are most susceptible to thermal annealing collected from the Taza-Guercif basin, Rif, and Middle Atlas of Morocco. Samples were chemically etched for very short time periods so as to evaluate only the oldest and most damaged zircon, which leaves younger zircons with relatively unaltered crystal lattices under-etched and therefore uncountable. While the primary findings of significant Pan-African and Hercynian cooling age populations dominate the data, there are unquestionably younger populations that could not be analyzed in the scope of this study. However, the retention of cooling ages from up to 600 Ma and older suggests that North Africa has experienced a relatively long-lived quiescence in terms of tectonothermal activity, at least in terms of processes creating thermal anomalies up to 300°C.

4.2 FUTURE APPLICATIONS FOR SEM-HDFT

Fission-track dating, among other thermochronological techniques, has become an increasingly viable tool in understanding shallow Earth processes. The time-temperature histories revealed through analyzing zircon and apatite have the potential to elucidate a number of important aspects of source-to-sink systems, including exhumation history, burial timing, changes in geothermal gradient, and sediment provenance.

The present study investigates an improvement in the applicability of ZFT dating, which has a thermal annealing temperature of ~240°C (Garver, 2002; Reiners et al., 2005); however the technique is transferable to the apatite fission-track system, which anneals at ~100°C (Reiners et al., 2005). Therefore, the expansion of the applicability of ZFT dating through the use of SEM-HDFT to assess thermal histories beyond the 300-

www.manaraa.com

400 Ma limit of optical fission-track analysis also increases the scope of apatite fission-track studies.

The improvements and increased age-range for fission-track dating afforded by the new SEM-HDFT technique may provide insight into a number of other geologic problems. One such application, based on the unique temperature range for the zircon fission-track system, may be improved calibration of the Conodont Alteration Index. Conodonts are small phosphatic biomineralized structures, believed to be the mouthparts of soft-bodied, nektobenthic chordates that are common in Paleozoic and Triassic marine carbonates (Peppe & Reiners, 2007). Conodonts are particularly helpful as a paleothermometer, as their coloration alters gradually and consistently when heated to temperatures between 50°C and >600°C, which is currently classified from values 1-8 on the Conodont Alteration Index and reflects post-depositional thermal alterations of the surrounding sediments. Zircon fission-track analyses on conondont host rocks may serve as a useful calibration method for the middle- to high-temperature indices, especially for Cambrian-age conodonts.

Another potential application for the recently improved fission-track analyses lies in the petroleum industry. Understanding the thermal history of rock formations—sedimentary formations in particular—is vital in understanding petroleum systems, as it can help constrain the timing of burial and ultimately the maturation hydrocarbons. In order for kerogen to produce oil and/or gas, it must be heated to approximately 60-150°C. Maximum temperature for oil-bearing formations is generally determined by observing the reflectance of vitrinite—an organic component of kerogen with a vitreous, or glassy appearance. Vitrinite reflectance, however, is only viable for assessing formations that

www.manaraa.com

are Silurian and younger, as vitrinite did not exist prior to the evolution of land plants (Schlumberger). The advancements made in fission-track analyses, therefore, could prove to be valuable in modeling the thermal histories of older, petroleum-bearing formations.

Recently, a number of commercial, Proterozoic-sourced petroleum accumulations have been explored in a number of countries. The Beetaloo Basin in Australia is among the oldest petroleum systems in the world, sourcing from the Mesoproterozoic Roper Group (1.4 Ga; Silverman & Ahlbrandt, 2011). Commercially viable, Proterozoic-sourced petroleum accumulations in Siberia, Oman, and China, with several fields containing >500 MBbl (million barrels) of oil and/or 3 Tcf (trillion cubic feet) of gas, provide further incentive to understand ancient thermal histories to facilitate the exploration of "older" petroleum systems (Craig et al., 2009). Additional potential and proven Precambrian source rocks include the Canadian Upper Huronian Series and its equivalents in SE Greenland, the Ukrainian Krivoy Series, and oil shales within the Russian Onega Basin (Craig et al., 2009). In the absence of vitrinite in pre-Silurian formations, fission-track analyses may now provide the insight necessary to properly model the thermal history and maturation of hydrocarbons.

www.manaraa.com

CHAPTER 5

CONCLUSION

A new technique in ZFT dating was employed in an attempt to elucidate the tectonic drivers of the Messinian salinity crisis in northwest Africa. Basin sediments from the Taza-Guercif basin, which sits along the southern margin of the Rifean Corridor in northern Morocco, were compared to two proximal mountain ranges to identify the predominant source area by means of a thermal signature related to the cooling histories of the sink and sources. While a distinct link to one source area over another (Rif vs. Middle Atlas) was not established, the cooling ages revealed a long-term history of thermal quiescence in northwest Africa. The two significant fission-track populations (319.1 ± 16.7 Ma, 607.2 ± 34.7 Ma), accounting for 85% of grains analyzed, imply that little to no thermal annealing has occurred following crystallization during the Hercynian and Pan-African orogenies, respectively. The relatively low errors coupled with the significance of the two crustal events in Earth's history reinforce the accuracy and applicability of the emerging SEM-HDFT technique as a thermochronologic and geochronologic tool. In addition, the protracted scope for zircon and/or apatite fission-track analyses may provide an increased ability to model paleothermometry, especially in determining thermal histories and maturity of petroleum systems.

www.manaraa.com

REFERENCES

Bernet, M., 2002., Exhuming the Alps through time: clues from detrital zircon fission-track ages. Ph.D dissertation, Yale University, New Haven, CT.

Bernet, M., Garver, J.I., 2005, Chapter 8: Fission-track analysis of Detrital zircon, In P.W. Reiners, and T. A. Ehlers, (eds.), Low-Temperature thermochronology: Techniques, Interpretations, and Applications, Reviews in Mineralogy and Geochemistry Series, v. 58, p. 205-237.

Bernini, M., Boccaletti, M., El Mokhtari, J., Gelati, R., Moratti, G., Papani, G., 1994, Geologic-structural map of the Taza-Guercif Neogene basin (North-eastern Morocco). Notes et Mémoires du Service Géologique du Maroc, v. 387.

Bernini, M., Boccaletti, M., Moratti, G., Papani, G., 2000, Structural development of the Taza-Guercif Basin as a constraint for the Middle Atlas Shear Zone tectonic evolution. Marine and Petroleum Geology, v 17, p. 391-408.

Begg, B.C., Griffin, W.L., Natapov, L.M., O'Reilley, S.Y., Grand, S.P., O'Neill, C.J., Hronsky, J.M.A., Djomani, Y.P., Swain, C.J., Deen, T., Bowden, P., 2009, The lithospheric architecture of Africa: Seismic tomography, mantle petrology, and tectonic evolution. Geosphere, v. 5, no. 1, p. 23-50

Brandon, M.T., Vance, J.A., 1992, Tectonic evolution of the Cenozoic Olympic subduction complex, Washington State, as deduced from fission track ages for detrital zircons. Am. J. Sci. 292:565–636.

Brandon, M.T., Roden-Tice, M.R., Garver, J.I., 1998, Late Cenozoic exhumation of the Cascadia accretionary wedge in the Olympic Mountains, northwest Washington State, Geological Society of America Bulletin, v 100, p. 985-1009.

Chalouan, A., Michard, A., Feinburg, H., Montigny, R., Saddiqi, O., 2001, The Rif mountain building (Morocco): a new tectonic scenario. Bulletin de la Société Géologique de France, v. 172, no. 5, pp. 603-616

www.manaraa.com

Chalouan, A., Michard, A., El Khadiri, Kh., Negro, F., Frizon de Lamotte, D., Soto, J.I., Saddiqi, O., 2008, Chapter 5: The Rif Belt, in Michard, A., Saddiqi, O., Chalouan, A., Frizon de Lamotte, D., (eds.), Continental Evolution: The Geology of Morocco: Structure, Stratigraphy, and Tectonics of the Africa-Atlantic-Mediterranean Triple Junction, v. 116 of Lecture Notes in Earth Science, Springer, 426 pp.

Craig, J., Thurow, J., Thusu, B., Whitham, A., Abutarruma, Y., 2009, Global Neoproterozoic Petroleum Systems: The Re-emerging Potential in North Africa, Geological Society of London, 309 p.

Fleischer, R.L., Price, P.B., Walker, R. M., 1975, Nuclear tracks in solids. Berkeley, University of California Press, 605 p.

Foster, D.A., Kohn, B.P., Gleadow, A. J., 1996, Sphene and zircon fission-track closure temperature revisited: empirical calibrations from 40Ar/39Ar diffusion studies on K-feldspar and biotite. International Workshop on Fission-Track Dating (University of Ghent, Aug. 26–30), Abstr. 37.

Garver, J.I., Kamp, P.J.J., 2002, Integration of zircon color and zircon fission-track zonation patterns in orogenic belts: application to the Southern Alps, New Zealand. Tectonophysics 349:203–219.

Garver, J.I., 2003, Etching zircon age standards for fission-track analysis. Radiation Measurements, v. 37, no. 1, pp. 47-53

Gelati, R., Moratti, G., Papani, G., 2000, The Late Cenozoic sedimentary succession of the Taza-Guercif Basin, South Rifean Corridor, Morocco, Marine and Petroleum Geology, v. 17, p. 373-390

Gehrels, G.W., Dickinson, W.R., Ross, G.M., Stewart, J.H., Howell, D.G., 1995, Detrital zircon reference for Cambrian to Triassic miogeoclinal strata of western North America. Geology 23:831–834.

Harrison, T.M., Armstrong, R.L., Naeser, C.W., Harakal, J.E., 1979, Geochronology and thermal history of the Coast Plutonic Complex, near Prince Rupert, British Columbia. Can. J. Earth Sci. 16:400–410.

Hurford, A.J., 1986, Cooling and uplift patterns in the Lepontine Alps south central Switzerland and age of vertical movement on the Insubric fault line. Contrib. Mineral. Petrol. 92:413–417.

Hsü, K. J., Montadert, L., Bernoulli, D., Cita, M. B., Erickson, A., Garrison, R. E., Kidd, R.B., Mèlierés, F, Muller, C, and Wright, R.C, 1977. History of the Mediterranean salinity crisis. Nature, 267:399-402.

www.manaraa.com

Krijgsman, W., Langereis, C.G., Zachariasse, W.J., Boccaletti, M., Morati, G., Gelati, R., Iaccarino, S., Papani, G., Villa, G., 1999, Late Neogene evolution of the Taza-Guercif Basin (Rifean Corridor Morocco) and implications for the Messinian salinity crisis, Marin Geology, v. 153, p. 147-160.

Krijgsman, W., Hilgen, F.J., Raffi, I., Sierro, F.J., Wilson, D.S., 1999, Chronology, causes and progression of the Messinian salinity crisis, Nature, v. 400, pp. 652-655.

Marsellos, A.E., Garver, J.I., 2010, Radiation damage and uranium concentration in zircon as assessed by Raman spectroscopy and neutron irradiation. American Mineralogist, v. 95, p. 1192–1201.

Montario, M., Garver, J.I., 2009, The Thermal Evolution of the Grenville Terrane Revealed through U-Pb and Fission-Track Analysis of Detrital Zircon from Cambro-Ordovician Quartz Arenites of the Potsdam and Galway Formations, Journal of Geology, v. 117, p. 595-614.

Paul, T.A., 1993, Transmission electron microscopy investigation of unetched fission tracks in fluorapatite—physical process of annealing. Nucl. Tracks Radiat. Meas. 21:507-511.

Paul, T.A., Fitzgerald, P.G., 1992, Transmission electron microscopic investigation of fission tracks in fluorapatite. Am. Min. 77:336-344.

Peppe, D.J., Reiners, P.W., 2007, Conodont (U-Th)/He thermochronology: Initial results, potential, and problems. Earth and Planetary Science Letters, no. 258, pp. 569-580

Price, P.B., Walker, R.M., 1963, Fossil tracks of charged particles in mica and the age of minerals. Journal of Geophysical Research. 68:4847-4862.

Reiners, P.W., Zhou, Z., Ehlers, T.A., Xu, C., Brandon, M.T., Donelick, R.A., Nicolescu, S., 2003, Postorogenic evolution of the Dabie Shan, eastern China, from (U-Th)/He and fission-track analysis. Am. J. Sci. 303:489–518.

Reiners, P.W., Ehlers, T.A., Zeitler, P.K., 2005, Past, Present, and Future of Thermochronology, Reviews in Mineralogy & Geochemistry, v. 58, pp. 1-18

Reiners, P.W., Brandon, M.T., 2006, Using thermochronology to understand orogenic erosion. Annual Review of Earth and Planetary Sciences, v. 34, p. 419–66

Rouchy, J.M., Caruso, A., 2006, The Messinian salinity crisis in the Mediterranean basin; A reassessment of the data and an integrated scenario. Sedimentary Geology, v. 188-189, p. 35-67.

www.manaraa.com

Schlumberger, 2013, Oilfield Glossary, Web accessed 28 Oct 2013 <http://www.glossary.oilfield.slb.com/en/Terms.aspx?LookIn=term%20name&filter=vitrinite%20reflectance>

Silverman, M., Ahlbrandt, T., 2011, Mesoproterozoic Unconventional Plays in the Beetaloo Basin, Australia: The World's Oldest Petroleum Systems, Seach and Discovery Article#10295, Web accessed 24 Oct 2013 <http://www.searchanddiscovery.com/documents/2011/10295silverman/ndx_silverman.pdf>

Tagami, T., O'Sullivan, P.B., 2005, Zircon Fission-Track Thermochronology and Applications to Fault Studies. In P.W. Reiners, and T. A. Ehlers, (eds.), Low-Temperature thermochronology: Techniques, Interpretations, and Applications, Reviews in Mineralogy and Geochemistry Series, v. 58, p. 95-122.

Wagner, G., Van den Haute, P., 1992, Fission-track dating: Solid Earth Sciences Library. Kluwer Academic Publishers, Amsterdam

Zaun, P.E., Wagner, G.A., 1985, Fission-track stability in zircons under geological conditions. Nuclear Tracks 10:303–307.

Zeck, H.P., Whitehouse, M.J., 1999, Hercynian, Pan-African, Proterozoic and Archeanion-microprobe zircon ages for a Betic-Rif core complex, Alpine belt, W Mediterranean - consequences for its P-T-t path. Contributions to Mineralogy and Petrology, no. 134, p. 134-149

Zeck, H.P., Whitehouse, M.J., 2002, Repeated age resetting in zircons from Hercynian–Alpine polymetamorphic schists (Betic–Rif tectonic belt, S. Spain) —a U–Th–Pb ion microprobe study, Chemical Geology, no. 182, p. 275-29

www.manaraa.com

APPENDIX A – ZETA CALIBRATION

www.manaraa.com

MEAN ZETA CALCULATION

TITLE: Taza-Guercif Basin, Morocco (SEM-HDFT)
OPERATOR NAME: Tyler Izykowski
DATE: 17 May 2013

RESULTS

Weighted Mean Zeta =	**321.9**
±1SE =	**10.6**
±2SE =	**21.2**

DATA

Irradiation		Age Standard	Measured Zeta (a cm^2 tk^{-1})		
Run Name	Position Number	Name	Zeta Value	Count SE	Total SE
U40Z	4.0	FCT-13	371.2	22.1	23.1
U40Z	44.0	FCT-14	273.7	40.0	40.3
U40Z	5.0	FCT-15	339.6	33.7	34.3
U43Z	34.0	BLK-21	355.7	55.6	55.7
U43Z	35.0	FCT-21	310.4	17.6	18.4
U43Z	36.0	FCT-36	298.1	17.6	18.4
U50Z	41.0	FCT-4	330.6	23.1	23.9

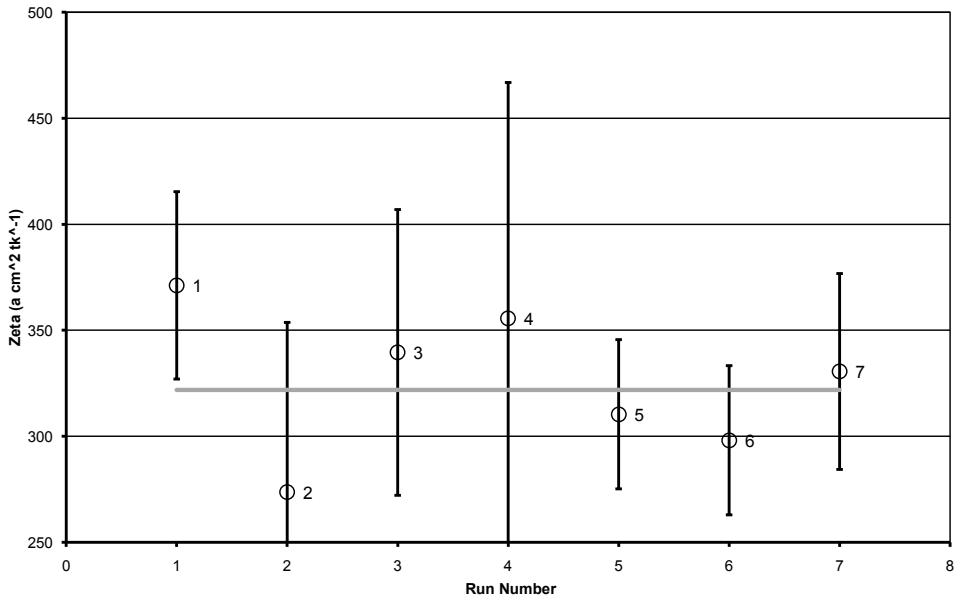

Note: This is the Excel replacement for ZetaMean (Mark Brandon, April, 2007). Individual zeta values are shown with 2SE error bars. The horizontal gray line indicates the weighted mean zeta value. Each data entry includes the zeta measurement plus two standard error estimates: the first represents only those uncertainties associated with the fission-track (FT) method (densities for spontaneous, induced, and fluence monitor), whereas the second includes the additional uncertainty associated with age of the age standard. The resulting mean zeta is calculated as a weighted average using count standard errors as weighting factors. (Count standard errors account for the collective uncertainties due to the measured induced, spontaneous, and monitor track densities.) In calculating the standard error, we first calculated a count-only standard error for the weighted mean and then add the standard error due to the age standard. This procedure accounts for the fact that the uncertainty associated with the age of the standard is common to all zeta measurements.

www.manaraa.com

==========Zfactor Program v. 1.2 (Brandon 3/18/95)==========
DATE/TIME: 05-22-2012/15:53:23 FILENAME:
C:\DOCUME~1\JOHNGA~1\DESKTOP\FTFOLD~1\TYLER\STANDA~1\B21_43Z.FTZ
BLK-21, U43Z-34, IZYKOWSKI, 22 May 2012

AGE (MA) AND STANDARD ERROR (MY) OF AGE STANDARD: 16.40 0.20
TRACK DENSITY FOR GLASS STANDARD (TRACKS/CM^2): 2.770E+05
RELATIVE STANDARD ERROR FOR GLASS DENSITY (%): 1.29
SIZE OF COUNTING SQUARE (CM^2): 4.420E-06

------ ZETA FOR GRAINS OF AGE STANDARD ------

Grain no.	RhoS (cm^-2)	(Ns)	RhoI (cm^-2)	(Ni)	Squares	Zeta (yr cm^2)	Grain-only SE	Total SE
1	7.999E+05	(8)	3.900E+06	(39)	2	577.99	224.5	224.6
2	8.999E+05	(9)	2.700E+06	(27)	2	355.69	137.0	137.0
3	1.332E+06	(10)	3.064E+06	(23)	2	272.69	103.4	103.4
4	1.600E+06	(9)	2.489E+06	(14)	1	184.43	78.8	78.9
5	1.244E+06	(7)	5.155E+06	(29)	1	491.19	206.9	207.0
6	2.715E+06	(12)	7.467E+06	(33)	1	326.05	110.0	110.1
POOLED	1.274E+06	(55)	3.821E+06	(165)	10	355.69	55.6	55.7
MEAN ZETA (using grain ratios)						320.28	55.7	55.9

CHI-SQUARED PROBABILITY (%): 39.2

MEAN (RhoS/RhoI) +/- 1 SE: 0.370 +/- 0.0642

==========Zfactor Program v. 1.2 (Brandon 3/18/95)==========
DATE/TIME: 02-23-2013/14:53:07 FILENAME:
C:\USERS\SENTERRA\DESKTOP\ZFT\IZYK\STANDA~1\FC4_50Z.FTZ
FCT_4,U50Z-41, Izykowski

AGE (MA) AND STANDARD ERROR (MY) OF AGE STANDARD: 27.90 0.50
TRACK DENSITY FOR GLASS STANDARD (TRACKS/CM^2): 2.949E+05
RELATIVE STANDARD ERROR FOR GLASS DENSITY (%): 1.38
SIZE OF COUNTING SQUARE (CM^2): 1.000E-06

------ ZETA FOR GRAINS OF AGE STANDARD ------

Grain no.	RhoS (cm^-2)	(Ns)	RhoI (cm^-2)	(Ni)	Squares	Zeta (yr cm^2)	Grain-only SE	Total SE
1	6.765E+04	(23)	1.353E+05	(46)	340	379.25	97.0	97.2
2	4.511E+04	(24)	9.211E+04	(49)	532	387.15	96.6	96.9
3	8.083E+04	(43)	1.071E+05	(57)	532	251.37	50.9	51.1
4	9.586E+04	(51)	1.316E+05	(70)	532	260.27	48.1	48.3
5	9.398E+04	(50)	1.711E+05	(91)	532	345.12	60.9	61.3
6	8.459E+04	(45)	1.391E+05	(74)	532	311.83	59.1	59.4
7	5.451E+04	(29)	1.165E+05	(62)	532	405.41	91.4	91.7
8	4.511E+04	(24)	9.962E+04	(53)	532	418.76	103.2	103.5
9	8.647E+04	(46)	1.541E+05	(82)	532	338.03	62.4	62.7
POOLED	7.289E+04	(335)	1.271E+05	(584)	4596	330.57	23.1	23.9
MEAN ZETA (using grain ratios)						333.86	22.0	22.8

CHI-SQUARED PROBABILITY (%): 62.9

MEAN (RhoS/RhoI) +/- 1 SE: 0.568 +/- 0.0366

www.manaraa.com

==========Zfactor Program v. 1.2 (Brandon 3/18/95)==========
DATE/TIME: 05-22-2012/16:17:05 FILENAME:
C:\DOCUME~1\JOHNGA~1\DESKTOP\FTFOLD~1\TYLER\STANDA~1\F13_40Z.FTZ
FCT_13,U40Z-4, Izykowski

AGE (MA) AND STANDARD ERROR (MY) OF AGE STANDARD: 27.90 0.50
TRACK DENSITY FOR GLASS STANDARD (TRACKS/CM^2): 3.026E+05
RELATIVE STANDARD ERROR FOR GLASS DENSITY (%): 1.77
SIZE OF COUNTING SQUARE (CM^2): 4.420E-06

------ ZETA FOR GRAINS OF AGE STANDARD ------

Grain no.	RhoS (cm^-2)	(Ns)	RhoI (cm^-2)	(Ni)	Squares	Zeta (yr cm^2)	Grain-only SE	Total SE
1	4.899E+06	(49)	7.999E+06	(80)	2	301.72	55.0	55.3
2	8.199E+06	(82)	1.750E+07	(175)	2	394.39	53.2	53.7
3	3.198E+06	(24)	5.995E+06	(45)	2	346.50	87.8	88.0
4	2.400E+06	(24)	4.399E+06	(44)	2	338.80	86.2	86.4
5	5.499E+06	(55)	9.899E+06	(99)	2	332.64	56.3	56.6
6	8.599E+06	(86)	1.810E+07	(181)	2	388.94	51.4	51.9
7	3.500E+06	(35)	6.999E+06	(70)	2	369.60	76.8	77.1
8	6.499E+06	(65)	1.740E+07	(174)	2	494.70	72.4	73.0
9	4.499E+06	(45)	6.599E+06	(66)	2	271.04	52.6	52.8
POOLED	5.313E+06	(465)	1.067E+07	(934)	20	371.19	22.1	23.1
MEAN ZETA (using grain ratios)						350.45	20.6	21.5

CHI-SQUARED PROBABILITY (%): 35.3

MEAN (RhoS/RhoI) +/- 1 SE: 0.527 +/- 0.0295

==========Zfactor Program v. 1.2 (Brandon 3/18/95)==========
DATE/TIME: 05-22-2012/16:15:11 FILENAME:
C:\DOCUME~1\JOHNGA~1\DESKTOP\FTFOLD~1\TYLER\STANDA~1\F14_40Z.FTZ
FCT_14,U40Z-44, Izykowski

AGE (MA) AND STANDARD ERROR (MY) OF AGE STANDARD: 27.90 0.50
TRACK DENSITY FOR GLASS STANDARD (TRACKS/CM^2): 2.577E+05
RELATIVE STANDARD ERROR FOR GLASS DENSITY (%): 1.30
SIZE OF COUNTING SQUARE (CM^2): 4.420E-06

------ ZETA FOR GRAINS OF AGE STANDARD ------

Grain no.	RhoS (cm^-2)	(Ns)	RhoI (cm^-2)	(Ni)	Squares	Zeta (yr cm^2)	Grain-only SE	Total SE
1	5.899E+06	(59)	2.900E+06	(29)	2	106.66	24.2	24.3
2	8.899E+06	(89)	1.280E+07	(128)	2	312.09	43.3	43.6
3	5.499E+06	(55)	7.099E+06	(71)	2	280.13	50.5	50.7
4	5.699E+06	(57)	6.999E+06	(70)	2	266.49	47.7	47.9
5	2.400E+06	(24)	4.000E+06	(40)	2	361.67	93.5	93.7
6	4.000E+06	(40)	4.299E+06	(43)	2	233.28	51.3	51.5
7	2.800E+06	(28)	4.100E+06	(41)	2	317.75	78.0	78.2
8	1.030E+07	(103)	6.299E+06	(63)	2	132.73	21.3	21.4
9	5.999E+06	(60)	1.240E+07	(124)	2	448.47	70.8	71.2
10	5.599E+06	(56)	1.080E+07	(108)	2	418.50	69.1	69.5
POOLED	5.709E+06	(571)	7.169E+06	(717)	23	272.49	15.7	16.4
MEAN ZETA (using grain ratios)						236.66	41.8	42.0

CHI-SQUARED PROBABILITY (%): 0.0

MEAN (RhoS/RhoI) +/- 1 SE: 0.917 +/- 0.1615

www.manaraa.com

==========Zfactor Program v. 1.2 (Brandon 3/18/95)==========
DATE/TIME: 05-22-2012/16:15:30 FILENAME:
C:\DOCUME~1\JOHNGA~1\DESKTOP\FTFOLD~1\TYLER\STANDA~1\F15_40Z.FTZ
FCT_15,U40Z-5, Izykowski

AGE (MA) AND STANDARD ERROR (MY) OF AGE STANDARD: 27.90 0.50
TRACK DENSITY FOR GLASS STANDARD (TRACKS/CM^2): 3.015E+05
RELATIVE STANDARD ERROR FOR GLASS DENSITY (%): 1.76
SIZE OF COUNTING SQUARE (CM^2): 4.420E-06

------ ZETA FOR GRAINS OF AGE STANDARD ------

Grain no.	RhoS (cm^-2)	(Ns)	RhoI (cm^-2)	(Ni)	Squares	Zeta (yr cm^2)	Grain-only SE	Total SE
1	5.199E+06	(52)	1.240E+07	(124)	2	442.29	73.5	73.9
2	7.499E+06	(75)	9.899E+06	(99)	2	244.83	37.7	38.0
3	3.500E+06	(35)	8.699E+06	(87)	2	461.04	92.6	93.0
4	8.532E+06	(48)	1.955E+07	(110)	1	425.05	73.9	74.3
5	7.821E+06	(44)	8.532E+06	(48)	1	202.34	42.4	42.5
6	7.699E+06	(77)	1.620E+07	(162)	2	390.22	54.4	54.9
7	6.399E+06	(64)	1.210E+07	(121)	2	350.67	54.5	54.9
8	5.729E+06	(43)	1.412E+07	(106)	2	457.22	83.1	83.5
9	5.899E+06	(59)	1.040E+07	(104)	2	326.94	53.6	53.9
10	6.799E+06	(68)	1.230E+07	(123)	2	335.49	51.0	51.4
POOLED	6.365E+06	(565)	1.221E+07	(1084)	20	355.85	19.5	20.5
MEAN ZETA (using grain ratios)						339.56	33.7	34.3

CHI-SQUARED PROBABILITY (%): 1.3

MEAN (RhoS/RhoI) +/- 1 SE: 0.546 +/- 0.0534

==========Zfactor Program v. 1.2 (Brandon 3/18/95)==========
DATE/TIME: 05-22-2012/16:16:03 FILENAME:
C:\DOCUME~1\JOHNGA~1\DESKTOP\FTFOLD~1\TYLER\STANDA~1\F21_43Z.FTZ
FCT_21,U43Z-35, Izykowski

AGE (MA) AND STANDARD ERROR (MY) OF AGE STANDARD: 27.90 0.50
TRACK DENSITY FOR GLASS STANDARD (TRACKS/CM^2): 2.762E+05
RELATIVE STANDARD ERROR FOR GLASS DENSITY (%): 1.29
SIZE OF COUNTING SQUARE (CM^2): 4.420E-06

------ ZETA FOR GRAINS OF AGE STANDARD ------

Grain no.	RhoS (cm^-2)	(Ns)	RhoI (cm^-2)	(Ni)	Squares	Zeta (yr cm^2)	Grain-only SE	Total SE
1	4.100E+06	(41)	5.199E+06	(52)	2	256.79	53.7	53.9
2	4.399E+06	(44)	4.499E+06	(45)	2	207.07	44.0	44.1
3	7.328E+06	(55)	1.466E+07	(110)	2	404.93	67.1	67.5
4	9.499E+06	(95)	1.250E+07	(125)	2	266.40	36.4	36.7
5	5.462E+06	(41)	8.660E+06	(65)	2	320.98	64.1	64.4
6	5.063E+06	(38)	8.393E+06	(63)	2	335.67	69.1	69.3
7	6.755E+06	(38)	1.102E+07	(62)	1	330.34	68.2	68.4
8	7.727E+06	(58)	9.326E+06	(70)	2	244.35	43.5	43.7
9	8.399E+06	(84)	1.240E+07	(124)	2	298.88	42.4	42.7
10	6.661E+06	(50)	1.572E+07	(118)	2	477.82	80.9	81.3
POOLED	6.542E+06	(544)	1.003E+07	(834)	19	310.40	17.6	18.4
MEAN ZETA (using grain ratios)						297.62	22.9	23.5

CHI-SQUARED PROBABILITY (%): 4.6

MEAN (RhoS/RhoI) +/- 1 SE: 0.680 +/- 0.0516

www.manaraa.com

==========Zfactor Program v. 1.2 (Brandon 3/18/95)==========
DATE/TIME: 05-22-2012/16:16:30 FILENAME:
C:\DOCUME~1\JOHNGA~1\DESKTOP\FTFOLD~1\TYLER\STANDA~1\F36_43Z.FTZ
FCT_36,U43Z-36, Izykowski

AGE (MA) AND STANDARD ERROR (MY) OF AGE STANDARD: 27.90 0.50
TRACK DENSITY FOR GLASS STANDARD (TRACKS/CM^2): 2.754E+05
RELATIVE STANDARD ERROR FOR GLASS DENSITY (%): 1.29
SIZE OF COUNTING SQUARE (CM^2): 4.420E-06

------ ZETA FOR GRAINS OF AGE STANDARD ------

Grain no.	RhoS (cm^-2)	(Ns)	RhoI (cm^-2)	(Ni)	Squares	Zeta (yr cm^2)	Grain-only SE	Total SE
1	8.393E+06	(63)	1.252E+07	(94)	2	302.97	49.5	49.8
2	7.599E+06	(76)	1.120E+07	(112)	2	299.24	44.6	45.0
3	6.399E+06	(36)	8.355E+06	(47)	1	265.10	58.8	59.0
4	4.999E+06	(50)	7.999E+06	(80)	2	324.89	58.7	59.0
5	5.196E+06	(39)	7.061E+06	(53)	2	275.94	58.3	58.5
6	6.262E+06	(47)	9.992E+06	(75)	2	324.02	60.4	60.7
7	6.129E+06	(46)	1.132E+07	(85)	2	375.21	68.8	69.2
8	1.013E+07	(57)	1.067E+07	(60)	1	213.74	39.6	39.8
9	4.699E+06	(47)	7.299E+06	(73)	2	315.38	59.1	59.4
10	4.299E+06	(43)	6.099E+06	(61)	2	288.05	57.5	57.7
POOLED	6.201E+06	(504)	9.104E+06	(740)	18	298.13	17.6	18.4
MEAN ZETA (using grain ratios)						292.49	15.1	16.0

CHI-SQUARED PROBABILITY (%): 75.7

MEAN (RhoS/RhoI) +/- 1 SE: 0.694 +/- 0.0347

www.manaraa.com

APPENDIX B – FLUENCE DATA

www.manaraa.com

==========Fluence Program v. 1.1 (Brandon 7/6/97)==========
DATE/TIME: 05-17-2012/15:53:30
IZYKOWSKI_U50Z_MAY_2012

=========INTERPOLATED TRACK DENSITY USING A PAIR OF GLASS STANDARDS=========

Monitor Label	Position	Distance(%)	Nd	RhoD (t/cm^2)	RE[RhoD](%)
FIRST MONITOR:	1	0.0	3008	3.460E+05	1.82
	2	1.9	3008	3.447E+05	1.80
	3	3.7	3008	3.434E+05	1.77
	4	5.6	3008	3.422E+05	1.74
	5	7.4	3008	3.409E+05	1.72
	6	9.3	3008	3.396E+05	1.69
	7	11.1	3008	3.383E+05	1.67
	8	13.0	3008	3.371E+05	1.64
	9	14.8	3008	3.358E+05	1.62
	10	16.7	3008	3.345E+05	1.59
	11	18.5	3008	3.332E+05	1.57
	12	20.4	3008	3.319E+05	1.54
	13	22.2	3008	3.307E+05	1.52
	14	24.1	3008	3.294E+05	1.50
	15	25.9	3009	3.281E+05	1.48
	16	27.8	3009	3.268E+05	1.46
	17	29.6	3009	3.256E+05	1.44
	18	31.5	3009	3.243E+05	1.42
	19	33.3	3009	3.230E+05	1.40
	20	35.2	3009	3.217E+05	1.39
	21	37.0	3009	3.204E+05	1.37
	22	38.9	3009	3.192E+05	1.36
	23	40.7	3009	3.179E+05	1.34
	24	42.6	3009	3.166E+05	1.33
	25	44.4	3009	3.153E+05	1.32
	26	46.3	3009	3.141E+05	1.31
	27	48.1	3009	3.128E+05	1.30
	28	50.0	3009	3.115E+05	1.30
	29	51.9	3009	3.102E+05	1.29
	30	53.7	3009	3.089E+05	1.29
	31	55.6	3009	3.077E+05	1.29
	32	57.4	3009	3.064E+05	1.29
	33	59.3	3009	3.051E+05	1.29
	34	61.1	3009	3.038E+05	1.30
	35	63.0	3009	3.026E+05	1.30
	36	64.8	3009	3.013E+05	1.31
	37	66.7	3009	3.000E+05	1.32
	38	68.5	3009	2.987E+05	1.34
	39	70.4	3009	2.974E+05	1.35
	40	72.2	3009	2.962E+05	1.37
	41	74.1	3009	2.949E+05	1.38
	42	75.9	3010	2.936E+05	1.40
	43	77.8	3010	2.923E+05	1.43
	44	79.6	3010	2.911E+05	1.45
	45	81.5	3010	2.898E+05	1.48
	46	83.3	3010	2.885E+05	1.50
	47	85.2	3010	2.872E+05	1.53
	48	87.0	3010	2.859E+05	1.56
	49	88.9	3010	2.847E+05	1.60

www.manaraa.com

==========Fluence Program v. 1.1 (Brandon 7/6/97)==========
DATE/TIME: 05-17-2012/15:53:30
IZYKOWSKI_U50Z_MAY_2012

=========INTERPOLATED TRACK DENSITY USING A PAIR OF GLASS STANDARDS=========

Monitor Label	Position	Distance(%)	Nd	RhoD (t/cm^2)	RE[RhoD](%)
	50	90.7	3010	2.834E+05	1.63
	51	92.6	3010	2.821E+05	1.67
	52	94.4	3010	2.808E+05	1.70
	53	96.3	3010	2.796E+05	1.74
	54	98.1	3010	2.783E+05	1.78
SECOND MONITOR:	55	100.0	3010	2.770E+05	1.82

www.manaraa.com

APPENDIX C – GRAIN AGE DATA

www.manaraa.com

==========ZetaAge Program v. 4.8 (Brandon 1/20/05)==========
DATE/TIME: 07-01-2013/17:42:07 FILENAME: E:\FINALR~1\TGB3A.TXT
TGB3A, U50Z-13

EFFECTIVE TRACK DENSITY FOR FLUENCE MONITOR (tracks/cm^2): 3.307E+05
RELATIVE ERROR (%): 1.52
EFFECTIVE URANIUM CONTENT OF MONITOR (ppm): 12.30
ZETA FACTOR AND STANDARD ERROR (yr cm^2): 321.90 10.60
SIZE OF COUNTER SQUARE (cm^2): 1.000E-08

------ GRAIN AGES IN ORIGINAL ORDER ------

Grain no.	RhoS (cm^-2)	(Ns)	RhoI (cm^-2)	(Ni)	Squares	U+/-2s	Grain Age	Age (Ma) --95% CI--	
1	5.25E+07	(107)	2.21E+07	(45)	204	820 245	125.1	87.8	181.2
2	9.91E+07	(336)	5.31E+06	(18)	339	197 92	916.6	590.4	1507.7
3	5.96E+07	(202)	1.21E+07	(41)	339	450 140	256.2	183.8	366.3
4	4.66E+07	(158)	4.42E+06	(15)	339	165 84	532.5	321.3	952.4
5	7.43E+07	(252)	3.54E+06	(12)	339	132 75	1018.5	599.3	1888.2
6	7.17E+07	(243)	7.08E+06	(24)	339	263 107	514.5	343.9	805.9
7	5.28E+07	(179)	9.14E+06	(31)	339	340 122	298.9	205.4	450.2
8	5.22E+07	(177)	5.60E+06	(19)	339	208 95	474.1	300.8	793.1
9	8.24E+07	(168)	4.41E+06	(9)	204	164 107	909.4	491.4	1901.7
10	4.40E+07	(149)	5.90E+06	(20)	339	219 97	382.2	242.8	636.1
11	8.61E+07	(292)	5.31E+06	(18)	339	197 92	803.8	515.0	1331.4
12	6.08E+07	(206)	7.08E+06	(24)	339	263 107	438.8	291.5	691.7
13	3.69E+07	(125)	1.09E+07	(37)	339	406 133	176.8	122.4	262.0
14	5.37E+07	(182)	8.26E+06	(28)	339	307 115	335.4	227.2	514.7
15	8.04E+07	(193)	7.92E+06	(19)	240	294 134	515.3	328.1	858.7
16	4.69E+07	(159)	6.49E+06	(22)	339	241 102	371.3	240.6	602.8
17	4.25E+07	(144)	3.54E+06	(12)	339	132 75	601.8	344.8	1155.8
18	4.72E+07	(160)	7.37E+06	(25)	339	274 109	330.2	218.5	521.1
19	5.49E+07	(186)	8.85E+06	(30)	339	329 120	320.4	219.5	484.8
20	4.69E+07	(159)	8.26E+06	(28)	339	307 115	294.0	198.0	453.5
21	4.93E+07	(167)	9.73E+06	(33)	339	362 126	262.8	181.7	392.4
22	6.05E+07	(205)	2.95E+06	(10)	339	110 68	993.7	556.1	1975.1
23	3.24E+07	(110)	9.73E+06	(33)	339	362 126	174.4	118.0	265.1
24	7.63E+07	(183)	8.33E+06	(20)	240	310 137	466.2	298.9	769.1
25	5.69E+07	(78)	8.76E+06	(12)	137	326 185	333.2	184.4	663.3
26	6.79E+07	(93)	6.57E+06	(9)	137	244 159	519.6	271.5	1135.1
27	4.37E+07	(148)	3.54E+06	(12)	339	132 75	617.7	354.4	1184.5
28	6.64E+07	(225)	6.78E+06	(23)	339	252 104	497.6	329.4	788.9
29	3.81E+07	(129)	5.01E+06	(17)	339	187 89	388.6	238.0	678.3
30	5.55E+07	(188)	7.37E+06	(25)	339	274 109	386.2	257.4	605.6
31	3.54E+07	(120)	3.54E+06	(12)	339	132 75	505.4	286.9	981.1
32	8.47E+07	(287)	7.96E+06	(27)	339	296 113	539.4	369.5	820.1
33	6.84E+07	(232)	7.08E+06	(24)	339	263 107	492.1	328.4	772.1
34	4.25E+07	(144)	1.06E+07	(36)	339	395 131	208.8	145.0	308.8
35	5.34E+07	(181)	5.01E+06	(17)	339	187 89	538.6	335.0	925.4
36	4.72E+07	(160)	8.55E+06	(29)	339	318 118	285.9	193.6	437.9
37	3.81E+07	(129)	4.13E+06	(14)	339	154 81	467.9	275.7	862.6
38	7.02E+07	(238)	5.31E+06	(18)	339	197 92	662.6	421.2	1108.2
39	2.63E+07	(89)	6.49E+06	(22)	339	241 102	210.6	132.3	351.3
40	3.27E+07	(111)	1.00E+07	(34)	339	373 128	170.9	116.2	258.3

www.manaraa.com

------ GRAIN AGES ORDERED WITH INCREASING AGE ------

Grain no.	RhoS (cm^-2)	(Ns)	RhoI (cm^-2)	(Ni)	Grain age (Ma) Age	--95% CI--		P(X2) (%)	Sum age (Ma) Age	--95% CI--	
1	5.25E+07	(107)	2.21E+07	(45)	125.1	87.8	181.2	100.0	125.1	87.8	181.2
40	3.27E+07	(111)	1.00E+07	(34)	170.9	116.2	258.3	23.0	144.7	111.1	188.2
23	3.24E+07	(110)	9.73E+06	(33)	174.4	118.0	265.1	34.8	153.6	122.9	191.9
13	3.69E+07	(125)	1.09E+07	(37)	176.8	122.4	262.0	46.0	159.5	131.1	193.9
34	4.25E+07	(144)	1.06E+07	(36)	208.8	145.0	308.8	35.4	169.2	141.7	201.9
39	2.63E+07	(89)	6.49E+06	(22)	210.6	132.3	351.3	38.4	173.7	146.8	205.6
3	5.96E+07	(202)	1.21E+07	(41)	256.2	183.8	366.3	12.7	187.6	160.5	219.0
21	4.93E+07	(167)	9.73E+06	(33)	262.8	181.7	392.4	6.9	196.5	169.6	227.7
36	4.72E+07	(160)	8.55E+06	(29)	285.9	193.6	437.9	3.3	205.1	178.0	236.1
20	4.69E+07	(159)	8.26E+06	(28)	294.0	198.0	453.5	1.7	212.6	185.5	243.6
7	5.28E+07	(179)	9.14E+06	(31)	298.9	205.4	450.2	0.9	220.0	192.8	250.9
19	5.49E+07	(186)	8.85E+06	(30)	320.4	219.5	484.8	0.4	227.7	200.4	258.6
18	4.72E+07	(160)	7.37E+06	(25)	330.2	218.5	521.1	0.2	233.9	206.4	264.9
25	5.69E+07	(78)	8.76E+06	(12)	333.2	184.4	663.3	0.2	236.7	209.2	267.8
14	5.37E+07	(182)	8.26E+06	(28)	335.4	227.2	514.7	0.1	242.8	215.2	273.9
16	4.69E+07	(159)	6.49E+06	(22)	371.3	240.6	602.8	0.0	248.8	221.0	280.1
10	4.40E+07	(149)	5.90E+06	(20)	382.2	242.8	636.1	0.0	254.2	226.2	285.7
30	5.55E+07	(188)	7.37E+06	(25)	386.2	257.4	605.6	0.0	260.6	232.3	292.3
29	3.81E+07	(129)	5.01E+06	(17)	388.6	238.0	678.3	0.0	264.7	236.2	296.5
12	6.08E+07	(206)	7.08E+06	(24)	438.8	291.5	691.7	0.0	272.2	243.4	304.4
24	7.63E+07	(183)	8.33E+06	(20)	466.2	298.9	769.1	0.0	279.0	249.7	311.5
37	3.81E+07	(129)	4.13E+06	(14)	467.9	275.7	862.6	0.0	283.5	254.0	316.3
8	5.22E+07	(177)	5.60E+06	(19)	474.1	300.8	793.1	0.0	289.5	259.7	322.6
33	6.84E+07	(232)	7.08E+06	(24)	492.1	328.4	772.1	0.0	297.2	267.0	330.7
28	6.64E+07	(225)	6.78E+06	(23)	497.6	329.4	788.9	0.0	304.3	273.7	338.2
31	3.54E+07	(120)	3.54E+06	(12)	505.4	286.9	981.1	0.0	308.0	277.2	342.1
6	7.17E+07	(243)	7.08E+06	(24)	514.5	343.9	805.9	0.0	315.2	284.0	349.7
15	8.04E+07	(193)	7.92E+06	(19)	515.3	328.1	858.7	0.0	320.6	289.1	355.4
26	6.79E+07	(93)	6.57E+06	(9)	519.6	271.5	1135.1	0.0	323.2	291.5	358.1
4	4.66E+07	(158)	4.42E+06	(15)	532.5	321.3	952.4	0.0	327.5	295.7	362.7
35	5.34E+07	(181)	5.01E+06	(17)	538.6	335.0	925.4	0.0	332.4	300.3	367.8
32	8.47E+07	(287)	7.96E+06	(27)	539.4	369.5	820.1	0.0	339.6	307.1	375.4
17	4.25E+07	(144)	3.54E+06	(12)	601.8	344.8	1155.8	0.0	343.7	311.0	379.7
27	4.37E+07	(148)	3.54E+06	(12)	617.7	354.4	1184.5	0.0	347.9	314.9	384.2
38	7.02E+07	(238)	5.31E+06	(18)	662.6	421.2	1108.2	0.0	354.9	321.5	391.7
11	8.61E+07	(292)	5.31E+06	(18)	803.8	515.0	1331.4	0.0	364.9	330.7	402.4
9	8.24E+07	(168)	4.41E+06	(9)	909.4	491.4	1901.7	0.0	370.9	336.4	409.0
2	9.91E+07	(336)	5.31E+06	(18)	916.6	590.4	1507.7	0.0	382.7	347.3	421.7
22	6.05E+07	(205)	2.95E+06	(10)	993.7	556.1	1975.1	0.0	390.1	354.1	429.6
5	7.43E+07	(252)	3.54E+06	(12)	1018.5	599.3	1888.2	0.0	399.0	362.3	439.2
POOL	5.51E+07	(6994)	7.12E+06	(904)				0.0	399.0	362.3	439.2

MEAN URANIUM CONCENTRATION +/-2SE (ppm): 265.0, 19.4

POOLED AGE WITH 68% CONF. INTERVAL(Ma): 399.0, 379.9 -- 419.1 (-19.1 +20.1)
95% CONF. INTERVAL(Ma): 362.3 -- 439.2 (-36.7 +40.2)
REDUCED CHI^2, DEGREES OF FREEDOM: 5.8889, 39
CHI^2 PROBABILITY: 0.0%

CENTRAL AGE WITH 68% CONF. INTERVAL(Ma): 377.5, 345.4 -- 412.4 (-32.1 +34.9)
95% CONF. INTERVAL(Ma): 317.1 -- 448.9 (-60.3 +71.4)
AGE DISPERSION (%): 48.1

CHI^2 AGE WITH 68% CONF. INTERVAL (Ma): 212.6, 198.3 -- 227.9 (-14.3 +15.3)
95% CONF. INTERVAL (Ma): 185.5 -- 243.6 (-27.1 +31.0)
NUMBER AND PERCENTAGE OF GRAINS: 10, 25

www.manaraa.com

==========ZetaAge Program v. 4.8 (Brandon 1/20/05)==========
DATE/TIME: 07-01-2013/17:42:19 FILENAME: E:\FINALR~1\TGB6B.TXT
TGB6B, U50Z-3

EFFECTIVE TRACK DENSITY FOR FLUENCE MONITOR (tracks/cm^2): 3.434E+05
RELATIVE ERROR (%): 1.77
EFFECTIVE URANIUM CONTENT OF MONITOR (ppm): 12.30
ZETA FACTOR AND STANDARD ERROR (yr cm^2): 321.90 10.60
SIZE OF COUNTER SQUARE (cm^2): 1.000E-08

------ GRAIN AGES IN ORIGINAL ORDER ------

Grain no.	RhoS (cm^-2)	(Ns)	RhoI (cm^-2)	(Ni)	Squares	U+/-2s		Grain Age	Age (Ma) --95% CI--	
1	4.60E+07	(244)	7.53E+06	(40)	531	270	85	327.6	235.7	467.2
2	4.42E+07	(255)	7.28E+06	(42)	577	261	81	326.1	236.5	461.0
3	4.58E+07	(243)	6.97E+06	(37)	531	250	82	351.9	250.7	508.3
4	3.09E+07	(164)	9.04E+06	(48)	531	324	94	185.7	134.5	261.4
5	3.52E+07	(187)	4.90E+06	(26)	531	175	68	383.7	257.2	596.9
6	1.71E+07	(41)	4.17E+06	(10)	240	149	92	220.1	110.6	488.8
7	6.06E+07	(206)	3.24E+06	(11)	340	116	68	947.5	542.3	1824.0
8	1.53E+07	(52)	7.06E+06	(24)	340	253	103	118.2	72.0	200.3
9	4.71E+07	(160)	6.18E+06	(21)	340	221	96	405.3	260.6	664.6
10	2.02E+07	(107)	4.52E+06	(24)	531	162	66	240.6	155.0	389.9
11	3.03E+07	(161)	4.90E+06	(26)	531	175	68	331.8	221.0	519.2

------ GRAIN AGES ORDERED WITH INCREASING AGE ------

Grain no.	RhoS (cm^-2)	(Ns)	RhoI (cm^-2)	(Ni)	Grain age (Ma) Age	--95% CI--		P(X2) (%)	Sum age (Ma) Age	--95% CI--	
8	1.53E+07	(52)	7.06E+06	(24)	118.2	72.0	200.3	100.0	118.2	72.0	200.3
4	3.09E+07	(164)	9.04E+06	(48)	185.7	134.5	261.4	12.3	163.0	124.1	213.9
6	1.71E+07	(41)	4.17E+06	(10)	220.1	110.6	488.8	21.0	170.2	131.8	219.6
10	2.02E+07	(107)	4.52E+06	(24)	240.6	155.0	389.9	16.2	186.4	148.9	233.3
2	4.42E+07	(255)	7.28E+06	(42)	326.1	236.5	461.0	0.7	226.5	187.3	273.9
1	4.60E+07	(244)	7.53E+06	(40)	327.6	235.7	467.2	0.2	248.3	209.4	294.4
11	3.03E+07	(161)	4.90E+06	(26)	331.8	221.0	519.2	0.2	258.7	220.2	303.9
3	4.58E+07	(243)	6.97E+06	(37)	351.9	250.7	508.3	0.1	272.7	234.5	317.0
5	3.52E+07	(187)	4.90E+06	(26)	383.7	257.2	596.9	0.1	283.4	245.2	327.4
9	4.71E+07	(160)	6.18E+06	(21)	405.3	260.6	664.6	0.0	292.2	253.9	336.2
7	6.06E+07	(206)	3.24E+06	(11)	947.5	542.3	1824.0	0.0	317.2	276.3	363.9
POOL	3.62E+07	(1820)	6.15E+06	(309)				0.0	317.2	276.3	363.9

MEAN URANIUM CONCENTRATION +/-2SE (ppm): 220.3, 26.3

POOLED AGE WITH 68% CONF. INTERVAL(Ma): 317.2, 295.6 -- 340.2 (-21.5 +23.1)
95% CONF. INTERVAL(Ma): 276.3 -- 363.9 (-40.8 +46.7)
REDUCED CHI^2, DEGREES OF FREEDOM: 4.9987, 10
CHI^2 PROBABILITY: 0.0%

CENTRAL AGE WITH 68% CONF. INTERVAL(Ma): 294.1, 255.4 -- 338.5 (-38.7 +44.4)
95% CONF. INTERVAL(Ma): 222.9 -- 387.3 (-71.2 +93.2)
AGE DISPERSION (%): 40.9

CHI^2 AGE WITH 68% CONF. INTERVAL (Ma): 186.4, 166.2 -- 209.1 (-20.2 +22.6)
95% CONF. INTERVAL (Ma): 148.9 -- 233.3 (-37.6 +46.9)
NUMBER AND PERCENTAGE OF GRAINS: 4, 36%

www.manaraa.com

==========ZetaAge Program v. 4.8 (Brandon 1/20/05)==========
DATE/TIME: 07-01-2013/17:42:33 FILENAME: E:\FINALR~1\TGB12A.TXT
TGB12A, U50Z-10

EFFECTIVE TRACK DENSITY FOR FLUENCE MONITOR (tracks/cm^2): 3.345E+05
RELATIVE ERROR (%): 1.59
EFFECTIVE URANIUM CONTENT OF MONITOR (ppm): 12.30
ZETA FACTOR AND STANDARD ERROR (yr cm^2): 321.90 10.60
SIZE OF COUNTER SQUARE (cm^2): 1.000E-08

------ GRAIN AGES IN ORIGINAL ORDER ------

Grain no.	RhoS (cm^-2)	(Ns)	RhoI (cm^-2)	(Ni)	Squares	U+/-2s	Grain Age	Age (Ma) --95% CI--	
1	5.31E+07	(180)	1.21E+07	(41)	339	445 139	231.5	165.2	332.3
2	4.42E+07	(150)	7.08E+06	(24)	339	260 106	326.2	213.9	520.7
3	4.19E+07	(142)	6.78E+06	(23)	339	249 103	322.3	209.3	520.4
4	5.34E+07	(181)	7.37E+06	(25)	339	271 108	376.4	250.5	591.2
5	5.60E+07	(190)	5.01E+06	(17)	339	184 88	570.5	355.6	977.8
6	4.16E+07	(141)	9.44E+06	(32)	339	347 122	232.1	158.5	350.8
7	4.42E+07	(150)	1.06E+07	(36)	339	390 130	219.8	153.0	324.6
8	6.64E+07	(225)	1.06E+07	(36)	339	390 130	326.8	231.4	475.5
9	5.78E+07	(196)	1.21E+07	(41)	339	445 139	251.6	180.2	360.1
10	4.96E+07	(168)	7.96E+06	(27)	339	293 112	325.0	218.2	503.9
11	8.43E+07	(172)	8.82E+06	(18)	204	324 151	491.2	308.1	833.5
12	5.66E+07	(192)	5.90E+06	(20)	339	217 96	493.7	317.2	812.8
13	4.13E+07	(140)	8.85E+06	(30)	339	325 118	245.5	166.0	375.6
14	1.05E+08	(357)	8.85E+06	(30)	339	325 118	608.0	425.9	899.3
15	4.22E+07	(143)	1.09E+07	(37)	339	401 132	204.2	142.3	300.7
16	5.25E+07	(178)	8.55E+06	(29)	339	315 116	320.8	218.3	489.4
17	5.08E+07	(122)	1.46E+07	(35)	240	536 181	184.4	126.5	276.1
18	3.98E+07	(135)	6.78E+06	(23)	339	249 103	306.8	198.7	496.5
19	5.40E+07	(74)	6.57E+06	(9)	137	242 157	421.7	217.1	935.6
20	6.64E+07	(91)	3.65E+06	(5)	137	134 115	887.0	392.4	2525.7
21	4.37E+07	(148)	6.49E+06	(22)	339	239 101	350.3	226.2	570.3
22	5.01E+07	(170)	7.08E+06	(24)	339	260 106	368.4	242.9	585.1
23	5.66E+07	(192)	9.14E+06	(31)	339	336 120	323.8	223.1	486.3
24	5.19E+07	(176)	9.73E+06	(33)	339	358 124	279.9	193.9	417.0
25	4.87E+07	(165)	5.31E+06	(18)	339	195 91	471.9	295.5	802.3
26	4.13E+07	(140)	7.08E+06	(24)	339	260 106	305.0	199.3	488.3
27	4.99E+07	(169)	7.67E+06	(26)	339	282 110	339.1	226.4	529.6
28	3.98E+07	(135)	6.78E+06	(23)	339	249 103	306.8	198.7	496.5
29	5.19E+07	(176)	3.24E+06	(11)	339	119 70	798.1	453.1	1555.2
30	4.88E+07	(117)	3.33E+06	(8)	240	123 84	729.9	375.2	1640.5
31	4.66E+07	(158)	8.85E+06	(30)	339	325 118	276.3	188.0	420.7
32	4.19E+07	(142)	1.36E+07	(46)	339	499 147	163.7	117.2	233.2
33	4.22E+07	(143)	6.19E+06	(21)	339	228 99	354.3	226.6	584.0
34	6.29E+07	(151)	1.00E+07	(24)	240	368 149	328.3	215.3	523.9
35	4.45E+07	(61)	1.46E+06	(2)	137	54 68	1370.9	421.2	7400.4

------ GRAIN AGES ORDERED WITH INCREASING AGE ------

Grain no.	RhoS (cm^-2)	(Ns)	RhoI (cm^-2)	(Ni)	Grain age (Ma) Age	--95% CI--		P(X2) (%)	Sum age (Ma) Age	--95% CI--	
32	4.19E+07	(142)	1.36E+07	(46)	163.7	117.2	233.2	100.0	163.7	117.2	233.2
17	5.08E+07	(122)	1.46E+07	(35)	184.4	126.5	276.1	63.5	172.4	133.5	222.4
15	4.22E+07	(143)	1.09E+07	(37)	204.2	142.3	300.7	66.6	182.5	147.4	225.9
7	4.42E+07	(150)	1.06E+07	(36)	219.8	153.0	324.6	65.4	191.4	158.4	231.2
1	5.31E+07	(180)	1.21E+07	(41)	231.5	165.2	332.3	61.8	200.0	168.6	237.1
6	4.16E+07	(141)	9.44E+06	(32)	232.1	158.5	350.8	66.8	204.6	174.3	240.0
13	4.13E+07	(140)	8.85E+06	(30)	245.5	166.0	375.6	67.3	209.5	180.0	243.8
9	5.78E+07	(196)	1.21E+07	(41)	251.6	180.2	360.1	64.5	215.4	186.7	248.5
31	4.66E+07	(158)	8.85E+06	(30)	276.3	188.0	420.7	56.7	221.1	192.6	253.7
24	5.19E+07	(176)	9.73E+06	(33)	279.9	193.9	417.0	50.3	226.6	198.4	258.7
26	4.13E+07	(140)	7.08E+06	(24)	305.0	199.3	488.3	41.8	231.6	203.4	263.6
28	3.98E+07	(135)	6.78E+06	(23)	306.8	198.7	496.5	36.7	236.0	207.8	267.8

www.manaraa.com

18	3.98E+07	(135)	6.78E+06	(23)	306.8	198.7	496.5	33.5	239.8	211.8	271.5
16	5.25E+07	(178)	8.55E+06	(29)	320.8	218.3	489.4	26.1	245.1	217.0	276.6
3	4.19E+07	(142)	6.78E+06	(23)	322.3	209.3	520.4	23.1	248.8	220.9	280.3
23	5.66E+07	(192)	9.14E+06	(31)	323.8	223.1	486.3	18.9	253.5	225.5	284.8
10	4.96E+07	(168)	7.96E+06	(27)	325.0	218.2	503.9	16.9	257.1	229.2	288.3
2	4.42E+07	(150)	7.08E+06	(24)	326.2	213.9	520.7	16.2	260.2	232.3	291.3
8	6.64E+07	(225)	1.06E+07	(36)	326.8	231.4	475.5	13.9	264.2	236.5	295.2
34	6.29E+07	(151)	1.00E+07	(24)	328.3	215.3	523.9	13.9	266.8	239.1	297.6
27	4.99E+07	(169)	7.67E+06	(26)	339.1	226.4	529.6	12.8	269.7	242.1	300.5
21	4.37E+07	(148)	6.49E+06	(22)	350.3	226.2	570.3	11.8	272.5	244.8	303.2
33	4.22E+07	(143)	6.19E+06	(21)	354.3	226.6	584.0	11.0	275.0	247.3	305.7
22	5.01E+07	(170)	7.08E+06	(24)	368.4	242.9	585.1	9.0	278.2	250.5	309.0
4	5.34E+07	(181)	7.37E+06	(25)	376.4	250.5	591.2	7.0	281.6	253.8	312.4
19	5.40E+07	(74)	6.57E+06	(9)	421.7	217.1	935.6	6.4	283.4	255.5	314.3
25	4.87E+07	(165)	5.31E+06	(18)	471.9	295.5	802.3	2.7	288.0	259.8	319.1
11	8.43E+07	(172)	8.82E+06	(18)	491.2	308.1	833.5	1.0	292.8	264.3	324.2
12	5.66E+07	(192)	5.90E+06	(20)	493.7	317.2	812.8	0.3	297.9	269.2	329.6
5	5.60E+07	(190)	5.01E+06	(17)	570.5	355.6	977.8	0.0	303.7	274.6	335.8
14	1.05E+08	(357)	8.85E+06	(30)	608.0	425.9	899.3	0.0	314.7	284.9	347.6
30	4.88E+07	(117)	3.33E+06	(8)	729.9	375.2	1640.5	0.0	318.8	288.7	352.0
29	5.19E+07	(176)	3.24E+06	(11)	798.1	453.1	1555.2	0.0	325.2	294.6	358.9
20	6.64E+07	(91)	3.65E+06	(5)	887.0	392.4	2525.7	0.0	328.7	297.9	362.7
35	4.45E+07	(61)	1.46E+06	(2)	1370.9	421.2	7400.4	0.0	331.5	300.4	365.8
POOL	5.14E+07	(5570)	8.14E+06	(881)				0.0	331.5	300.4	365.8

MEAN URANIUM CONCENTRATION +/-2SE (ppm): 299.2, 22.3

POOLED AGE WITH 68% CONF. INTERVAL(Ma):	331.5,	315.3 -- 348.6	(-16.2	+17.1)
95% CONF. INTERVAL(Ma):		300.4 -- 365.8	(-31.1	+34.2)
REDUCED CHI^2, DEGREES OF FREEDOM:	3.2092,	34		
CHI^2 PROBABILITY:	0.0%			
CENTRAL AGE WITH 68% CONF. INTERVAL(Ma):	332.6,	309.3 -- 357.6	(-23.3	+25.0)
95% CONF. INTERVAL(Ma):		288.5 -- 383.2	(-44.1	+50.6)
AGE DISPERSION (%):	31.4			
CHI^2 AGE WITH 68% CONF. INTERVAL (Ma):	288.0,	273.2 -- 303.4	(-14.7	+15.5)
95% CONF. INTERVAL (Ma):		259.8 -- 319.1	(-28.1	+31.1)
NUMBER AND PERCENTAGE OF GRAINS:	27,	77%		

www.manaraa.com

==========ZetaAge Program v. 4.8 (Brandon 1/20/05)==========
DATE/TIME: 07-01-2013/17:42:43 FILENAME: E:\FINALR~1\TGB14B.TXT
TGB14B, U50Z-6

EFFECTIVE TRACK DENSITY FOR FLUENCE MONITOR (tracks/cm^2): 3.396E+05
RELATIVE ERROR (%): 1.69
EFFECTIVE URANIUM CONTENT OF MONITOR (ppm): 12.30
ZETA FACTOR AND STANDARD ERROR (yr cm^2): 321.90 10.60
SIZE OF COUNTER SQUARE (cm^2): 1.000E-08

------ GRAIN AGES IN ORIGINAL ORDER ------

Grain no.	RhoS (cm^-2)	(Ns)	RhoI (cm^-2)	(Ni)	Squares	U+/-2s	Grain Age	Age (Ma) --95% CI--	
1	6.64E+07	(225)	1.36E+07	(46)	339	491 145	261.2	190.7	365.7
2	1.95E+07	(66)	3.83E+06	(13)	339	139 76	269.0	149.7	526.8
3	2.12E+07	(72)	5.90E+06	(20)	339	214 95	192.7	117.3	332.7
4	7.67E+07	(260)	6.19E+06	(21)	339	224 97	639.1	418.9	1026.9
5	5.40E+07	(183)	7.67E+06	(26)	339	278 108	371.7	249.0	578.7
6	4.45E+07	(151)	4.72E+06	(16)	339	171 84	491.9	300.0	865.7
7	5.22E+07	(177)	1.33E+07	(45)	339	481 143	210.9	152.1	298.7
8	4.69E+07	(159)	1.36E+07	(46)	339	491 145	185.7	133.7	263.4
9	8.17E+07	(277)	3.83E+06	(13)	339	139 76	1058.8	636.5	1905.6
10	8.29E+07	(281)	8.55E+06	(29)	339	310 115	506.5	350.4	760.0
11	5.66E+07	(192)	5.90E+06	(20)	339	214 95	500.9	321.8	824.4
12	5.69E+07	(193)	5.31E+06	(18)	339	192 90	556.5	350.8	939.2
13	4.63E+07	(157)	9.73E+06	(33)	339	353 122	253.9	175.1	380.0

------ GRAIN AGES ORDERED WITH INCREASING AGE ------

Grain no.	RhoS (cm^-2)	(Ns)	RhoI (cm^-2)	(Ni)	Grain age (Ma) Age	--95% CI--		P(X2) (%)	Sum age (Ma) Age	--95% CI--	
8	4.69E+07	(159)	1.36E+07	(46)	185.7	133.7	263.4	100.0	185.7	133.7	263.4
3	2.12E+07	(72)	5.90E+06	(20)	192.7	117.3	332.7	89.3	187.5	141.9	247.5
7	5.22E+07	(177)	1.33E+07	(45)	210.9	152.1	298.7	85.8	197.2	158.5	245.2
13	4.63E+07	(157)	9.73E+06	(33)	253.9	175.1	380.0	63.6	210.4	173.4	255.3
1	6.64E+07	(225)	1.36E+07	(46)	261.2	190.7	365.7	53.1	222.9	187.8	264.4
2	1.95E+07	(66)	3.83E+06	(13)	269.0	149.7	526.8	60.9	226.0	191.4	266.9
5	5.40E+07	(183)	7.67E+06	(26)	371.7	249.0	578.7	16.8	242.9	207.5	284.3
6	4.45E+07	(151)	4.72E+06	(16)	491.9	300.0	865.7	1.7	259.8	223.0	302.4
11	5.66E+07	(192)	5.90E+06	(20)	500.9	321.8	824.4	0.1	278.5	240.4	322.5
10	8.29E+07	(281)	8.55E+06	(29)	506.5	350.4	760.0	0.0	301.6	262.0	346.9
12	5.69E+07	(193)	5.31E+06	(18)	556.5	350.8	939.2	0.0	316.8	276.3	363.1
4	7.67E+07	(260)	6.19E+06	(21)	639.1	418.9	1026.9	0.0	337.9	295.8	385.8
9	8.17E+07	(277)	3.83E+06	(13)	1058.8	636.5	1905.6	0.0	366.9	322.0	417.9
POOL	5.43E+07	(2393)	7.85E+06	(346)				0.0	366.9	322.0	417.9

MEAN URANIUM CONCENTRATION +/-2SE (ppm): 284.4, 32.0

POOLED AGE WITH 68% CONF. INTERVAL(Ma): 366.9, 343.3 -- 392.1 (-23.6 +25.2)
95% CONF. INTERVAL(Ma): 322.0 -- 417.9 (-44.9 +50.9)
REDUCED CHI^2, DEGREES OF FREEDOM: 6.6575, 12
CHI^2 PROBABILITY: 0.0%

CENTRAL AGE WITH 68% CONF. INTERVAL(Ma): 345.0, 300.4 -- 396.1 (-44.6 +51.1)
95% CONF. INTERVAL(Ma): 262.8 -- 451.9 (-82.1 +106.9)
AGE DISPERSION (%): 44.6

CHI^2 AGE WITH 68% CONF. INTERVAL (Ma): 259.8, 240.3 -- 280.7 (-19.4 +21.0)
95% CONF. INTERVAL (Ma): 223.0 -- 302.4 (-36.7 +42.7)
NUMBER AND PERCENTAGE OF GRAINS: 8, 62%

www.manaraa.com

==========ZetaAge Program v. 4.8 (Brandon 1/20/05)==========
DATE/TIME: 07-01-2013/17:41:26 FILENAME: E:\FINALR~1\RF2A.TXT
RF2A, U50Z-27

EFFECTIVE TRACK DENSITY FOR FLUENCE MONITOR (tracks/cm^2): 3.128E+05
RELATIVE ERROR (%): 1.30
EFFECTIVE URANIUM CONTENT OF MONITOR (ppm): 12.30
ZETA FACTOR AND STANDARD ERROR (yr cm^2): 321.90 10.60
SIZE OF COUNTER SQUARE (cm^2): 1.000E-08

------ GRAIN AGES IN ORIGINAL ORDER ------

Grain no.	RhoS (cm^-2)	(Ns)	RhoI (cm^-2)	(Ni)	Squares	U+/-2s	Grain Age	Age (Ma) --95% CI--	
1	5.25E+07	(178)	5.60E+06	(19)	339	220 100	451.8	286.6	756.3
2	6.17E+07	(209)	6.78E+06	(23)	339	267 110	439.3	289.9	698.9
3	3.75E+07	(127)	1.59E+07	(54)	339	626 170	117.1	84.8	164.0
4	6.37E+07	(216)	6.49E+06	(22)	339	255 108	473.2	310.3	759.4
5	7.82E+07	(265)	1.39E+07	(47)	339	545 159	277.0	204.0	384.6
6	1.21E+08	(411)	1.06E+07	(36)	339	418 139	548.4	395.5	783.4
7	5.72E+07	(194)	1.09E+07	(37)	339	429 141	257.8	182.2	375.3
8	3.27E+07	(111)	2.65E+06	(9)	339	104 68	583.5	307.9	1262.2
9	6.25E+07	(212)	7.37E+06	(25)	339	290 115	411.1	275.2	642.2
10	5.19E+07	(176)	4.13E+06	(14)	339	162 85	597.6	357.0	1085.5
11	4.31E+07	(146)	6.78E+06	(23)	339	267 110	310.1	201.6	500.5
12	6.93E+07	(235)	4.42E+06	(15)	339	174 89	736.9	451.9	1293.7

------ GRAIN AGES ORDERED WITH INCREASING AGE ------

Grain no.	RhoS (cm^-2)	(Ns)	RhoI (cm^-2)	(Ni)	Grain age (Ma) Age	--95% CI--		P(X2) (%)	Sum age (Ma) Age	--95% CI--	
3	3.75E+07	(127)	1.59E+07	(54)	117.1	84.8	164.0	100.0	117.1	84.8	164.0
7	5.72E+07	(194)	1.09E+07	(37)	257.8	182.2	375.3	0.1	174.5	137.3	221.6
5	7.82E+07	(265)	1.39E+07	(47)	277.0	204.0	384.6	0.0	209.7	172.6	254.7
11	4.31E+07	(146)	6.78E+06	(23)	310.1	201.6	500.5	0.0	224.4	187.2	268.8
9	6.25E+07	(212)	7.37E+06	(25)	411.1	275.2	642.2	0.0	250.1	211.2	295.8
2	6.17E+07	(209)	6.78E+06	(23)	439.3	289.9	698.9	0.0	271.4	231.4	318.2
1	5.25E+07	(178)	5.60E+06	(19)	451.8	286.6	756.3	0.0	286.9	246.1	334.3
4	6.37E+07	(216)	6.49E+06	(22)	473.2	310.3	759.4	0.0	303.7	262.2	351.7
6	1.21E+08	(411)	1.06E+07	(36)	548.4	395.5	783.4	0.0	335.3	291.9	385.0
8	3.27E+07	(111)	2.65E+06	(9)	583.5	307.9	1262.2	0.0	343.3	299.4	393.4
10	5.19E+07	(176)	4.13E+06	(14)	597.6	357.0	1085.5	0.0	355.3	310.7	406.1
12	6.93E+07	(235)	4.42E+06	(15)	736.9	451.9	1293.7	0.0	373.8	327.8	426.0
POOL	6.10E+07	(2480)	7.96E+06	(324)				0.0	373.8	327.8	426.0

MEAN URANIUM CONCENTRATION +/-2SE (ppm): 313.2, 35.7

POOLED AGE WITH 68% CONF. INTERVAL(Ma): 373.8, 349.6 -- 399.6 (-24.2 +25.8)
95% CONF. INTERVAL(Ma): 327.8 -- 426.0 (-46.0 +52.2)
REDUCED CHI^2, DEGREES OF FREEDOM: 8.0936, 11
CHI^2 PROBABILITY: 0.0%

CENTRAL AGE WITH 68% CONF. INTERVAL(Ma): 363.1, 307.2 -- 428.8 (-55.9 +65.7)
95% CONF. INTERVAL(Ma): 261.5 -- 502.6 (-101.6 +139.6)
AGE DISPERSION (%): 54.3

CHI^2 AGE WITH 68% CONF. INTERVAL (Ma): 117.1, 98.7 -- 139.6 (-18.5 +22.5)
95% CONF. INTERVAL (Ma): 84.8 -- 164.0 (-32.3 +46.9)
NUMBER AND PERCENTAGE OF GRAINS: 1, 8%

www.manaraa.com

==========ZetaAge Program v. 4.8 (Brandon 1/20/05)==========
DATE/TIME: 07-01-2013/17:41:40 FILENAME: E:\FINALR~1\RF3A.TXT
RF3A, U50Z-30

EFFECTIVE TRACK DENSITY FOR FLUENCE MONITOR (tracks/cm^2): 3.089E+05
RELATIVE ERROR (%): 1.29
EFFECTIVE URANIUM CONTENT OF MONITOR (ppm): 12.30
ZETA FACTOR AND STANDARD ERROR (yr cm^2): 321.90 10.60
SIZE OF COUNTER SQUARE (cm^2): 1.000E-08

------ GRAIN AGES IN ORIGINAL ORDER ------

Grain no.	RhoS (cm^-2)	(Ns)	RhoI (cm^-2)	(Ni)	Squares	U+/-2s	Grain Age	Age (Ma) --95% CI--	
1	1.98E+07	(66)	3.89E+06	(13)	334	155 84	245.2	136.4	480.7
2	2.46E+07	(32)	6.15E+06	(8)	130	245 168	193.0	89.1	481.3
3	3.74E+07	(198)	3.97E+06	(21)	529	158 68	449.4	291.4	731.6
4	4.78E+07	(253)	7.37E+06	(39)	529	294 94	313.6	225.3	448.7
5	4.74E+07	(251)	8.51E+06	(45)	529	339 101	270.7	198.0	378.9
6	5.29E+07	(280)	4.73E+06	(25)	529	188 75	531.0	358.9	821.4
7	1.44E+07	(48)	4.19E+06	(14)	334	167 88	166.9	91.7	326.6
8	3.59E+07	(190)	5.86E+06	(31)	529	233 83	296.4	204.2	445.7
9	1.14E+07	(38)	7.78E+06	(26)	334	310 121	72.1	42.8	123.5
10	5.14E+07	(272)	3.40E+06	(18)	529	135 63	704.9	450.0	1174.0
11	3.46E+07	(183)	1.46E+07	(77)	529	580 133	116.7	88.9	153.1
12	3.88E+07	(205)	3.02E+06	(16)	529	120 59	602.0	371.7	1046.5

------ GRAIN AGES ORDERED WITH INCREASING AGE ------

Grain no.	RhoS (cm^-2)	(Ns)	RhoI (cm^-2)	(Ni)	Grain age (Ma) Age	--95% CI--		P(X2) (%)	Sum age (Ma) Age	--95% CI--	
9	1.14E+07	(38)	7.78E+06	(26)	72.1	42.8	123.5	100.0	72.1	42.8	123.5
11	3.46E+07	(183)	1.46E+07	(77)	116.7	88.9	153.1	9.0	105.5	82.9	134.3
7	1.44E+07	(48)	4.19E+06	(14)	166.9	91.7	326.6	8.1	113.0	90.2	141.6
2	2.46E+07	(32)	6.15E+06	(8)	193.0	89.1	481.3	7.2	118.3	95.2	147.1
1	1.98E+07	(66)	3.89E+06	(13)	245.2	136.4	480.7	1.2	130.6	106.3	160.3
5	4.74E+07	(251)	8.51E+06	(45)	270.7	198.0	378.9	0.0	165.4	138.6	197.3
8	3.59E+07	(190)	5.86E+06	(31)	296.4	204.2	445.7	0.0	184.7	156.9	217.5
4	4.78E+07	(253)	7.37E+06	(39)	313.6	225.3	448.7	0.0	204.9	176.1	238.3
3	3.74E+07	(198)	3.97E+06	(21)	449.4	291.4	731.6	0.0	224.2	193.8	259.2
6	5.29E+07	(280)	4.73E+06	(25)	531.0	358.9	821.4	0.0	250.6	218.0	288.0
12	3.88E+07	(205)	3.02E+06	(16)	602.0	371.7	1046.5	0.0	269.2	235.0	308.3
10	5.14E+07	(272)	3.40E+06	(18)	704.9	450.0	1174.0	0.0	293.8	257.4	335.2
POOL	3.76E+07	(2016)	6.21E+06	(333)				0.0	293.8	257.4	335.2

MEAN URANIUM CONCENTRATION +/-2SE (ppm): 247.2, 27.8

POOLED AGE WITH 68% CONF. INTERVAL(Ma): 293.8, 274.7 -- 314.3 (-19.1 +20.5)
95% CONF. INTERVAL(Ma): 257.4 -- 335.2 (-36.4 +41.4)
REDUCED CHI^2, DEGREES OF FREEDOM: 11.8036, 11
CHI^2 PROBABILITY: 0.0%

CENTRAL AGE WITH 68% CONF. INTERVAL(Ma): 247.5, 203.1 -- 301.3 (-44.3 +53.8)
95% CONF. INTERVAL(Ma): 168.0 -- 363.6 (-79.5 +116.1)
AGE DISPERSION (%): 64.5

CHI^2 AGE WITH 68% CONF. INTERVAL (Ma): 130.6, 117.6 -- 145.0 (-13.0 +14.4)
95% CONF. INTERVAL (Ma): 106.3 -- 160.3 (-24.3 +29.7)
NUMBER AND PERCENTAGE OF GRAINS: 5, 42%

www.manaraa.com

==========ZetaAge Program v. 4.8 (Brandon 1/20/05)==========
DATE/TIME: 07-01-2013/17:41:52 FILENAME: E:\FINALR~1\RF4A.TXT
RF4A, U50Z-33

EFFECTIVE TRACK DENSITY FOR FLUENCE MONITOR (tracks/cm^2): 3.051E+05
RELATIVE ERROR (%): 1.29
EFFECTIVE URANIUM CONTENT OF MONITOR (ppm): 12.30
ZETA FACTOR AND STANDARD ERROR (yr cm^2): 321.90 10.60
SIZE OF COUNTER SQUARE (cm^2): 1.000E-08

------ GRAIN AGES IN ORIGINAL ORDER ------

Grain no.	RhoS (cm^-2)	(Ns)	RhoI (cm^-2)	(Ni)	Squares	U+/-2s	Grain Age	Age (Ma) --95% CI--	
1	3.92E+07	(133)	5.60E+06	(19)	339	226 103	332.5	208.1	563.9
2	5.28E+07	(179)	5.90E+06	(20)	339	238 105	422.2	270.2	698.2
3	6.91E+07	(141)	5.39E+06	(11)	204	217 128	592.8	332.3	1176.2
4	9.82E+07	(333)	1.47E+07	(50)	339	595 168	318.1	237.6	435.0
5	5.87E+07	(199)	1.47E+06	(5)	339	59 51	1660.9	774.7	4286.1
6	4.93E+07	(167)	2.95E+06	(10)	339	119 73	760.9	420.6	1542.3
7	5.96E+07	(202)	6.78E+06	(23)	339	274 113	414.9	273.4	661.3
8	3.78E+07	(128)	5.01E+06	(17)	339	202 97	356.6	218.2	623.6
9	7.94E+07	(162)	1.13E+07	(23)	204	455 188	334.9	218.7	538.4
10	7.99E+07	(271)	6.49E+06	(22)	339	262 111	574.4	379.6	914.1
11	8.05E+07	(273)	3.83E+06	(13)	339	155 84	946.0	566.9	1713.4

------ GRAIN AGES ORDERED WITH INCREASING AGE ------

Grain no.	RhoS (cm^-2)	(Ns)	RhoI (cm^-2)	(Ni)	Grain age (Ma) Age	--95% CI--		P(X2) (%)	Sum age (Ma) Age	--95% CI--	
4	9.82E+07	(333)	1.47E+07	(50)	318.1	237.6	435.0	100.0	318.1	237.6	435.0
1	3.92E+07	(133)	5.60E+06	(19)	332.5	208.1	563.9	86.3	321.5	248.9	414.5
9	7.94E+07	(162)	1.13E+07	(23)	334.9	218.7	538.4	97.2	325.3	260.0	406.4
8	3.78E+07	(128)	5.01E+06	(17)	356.6	218.2	623.6	98.1	330.6	268.8	406.3
7	5.96E+07	(202)	6.78E+06	(23)	414.9	273.4	661.3	88.9	345.8	286.0	417.6
2	5.28E+07	(179)	5.90E+06	(20)	422.2	270.2	698.2	87.0	356.3	298.1	425.3
10	7.99E+07	(271)	6.49E+06	(22)	574.4	379.6	914.1	37.6	384.7	325.4	454.3
3	6.91E+07	(141)	5.39E+06	(11)	592.8	332.3	1176.2	27.7	397.7	338.0	467.5
6	4.93E+07	(167)	2.95E+06	(10)	760.9	420.6	1542.3	9.8	417.3	356.1	488.7
11	8.05E+07	(273)	3.83E+06	(13)	946.0	566.9	1713.4	0.5	452.3	387.9	527.0
5	5.87E+07	(199)	1.47E+06	(5)	1660.9	774.7	4286.1	0.0	484.7	416.6	563.4
POOL	6.33E+07	(2188)	6.16E+06	(213)				0.0	484.7	416.6	563.4

MEAN URANIUM CONCENTRATION +/-2SE (ppm): 248.3, 34.6

POOLED AGE WITH 68% CONF. INTERVAL(Ma): 484.7, 448.7 -- 523.4 (-36.0 +38.7)
95% CONF. INTERVAL(Ma): 416.6 -- 563.4 (-68.1 +78.7)
REDUCED CHI^2, DEGREES OF FREEDOM: 3.6449, 10
CHI^2 PROBABILITY: 0.0%

CENTRAL AGE WITH 68% CONF. INTERVAL(Ma): 488.4, 428.6 -- 556.1 (-59.7 +67.7)
95% CONF. INTERVAL(Ma): 378.0 -- 629.5 (-110.4 +141.1)
AGE DISPERSION (%): 35.7

CHI^2 AGE WITH 68% CONF. INTERVAL (Ma): 417.3, 384.9 -- 452.4 (-32.4 +35.0)
95% CONF. INTERVAL (Ma): 356.1 -- 488.7 (-61.2 +71.3)
NUMBER AND PERCENTAGE OF GRAINS: 9, 82%

www.manaraa.com

==========ZetaAge Program v. 4.8 (Brandon 1/20/05)==========
DATE/TIME: 07-01-2013/17:47:39 FILENAME: E:\FINALR~1\BR2AX.TXT
BR2A, U50Z-26

EFFECTIVE TRACK DENSITY FOR FLUENCE MONITOR (tracks/cm^2): 3.141E+05
RELATIVE ERROR (%): 1.31
EFFECTIVE URANIUM CONTENT OF MONITOR (ppm): 12.30
ZETA FACTOR AND STANDARD ERROR (yr cm^2): 321.90 10.60
SIZE OF COUNTER SQUARE (cm^2): 1.000E-08

------ GRAIN AGES IN ORIGINAL ORDER ------

Grain no.	RhoS (cm^-2)	(Ns)	RhoI (cm^-2)	(Ni)	Squares	U+/-2s	Grain Age	Age (Ma) --95% CI--	
1	4.48E+07	(161)	5.01E+06	(18)	359	196 91	433.6	271.1	738.9
2	4.51E+07	(162)	5.29E+06	(19)	359	207 94	414.2	261.7	696.1
3	2.20E+07	(79)	6.41E+06	(23)	359	251 104	170.5	107.0	283.5
4	3.01E+07	(108)	1.95E+06	(7)	359	76 56	721.4	355.7	1732.1
5	1.89E+07	(68)	5.85E+06	(21)	359	229 99	160.8	98.3	275.4
6	4.26E+07	(153)	4.18E+06	(15)	359	164 83	491.4	295.9	881.4
7	3.48E+07	(125)	5.01E+06	(18)	359	196 91	339.3	209.6	584.8
8	5.15E+07	(105)	6.86E+06	(14)	204	269 141	364.8	212.5	680.6
9	5.74E+07	(206)	8.64E+06	(31)	359	338 121	326.0	225.3	488.7
10	8.02E+07	(288)	4.18E+06	(15)	359	164 83	895.5	553.8	1554.6
11	5.04E+07	(181)	5.85E+06	(21)	359	229 99	418.8	270.6	684.0
12	7.86E+07	(187)	5.88E+06	(14)	238	230 121	635.6	380.7	1150.8
13	4.79E+07	(115)	5.42E+06	(13)	240	212 116	427.7	246.5	812.4
14	2.98E+07	(101)	5.31E+06	(18)	339	208 97	275.6	168.4	479.9
15	2.25E+07	(54)	3.33E+06	(8)	240	131 90	327.0	159.3	781.4

------ GRAIN AGES ORDERED WITH INCREASING AGE ------

Grain no.	RhoS (cm^-2)	(Ns)	RhoI (cm^-2)	(Ni)	Grain age (Ma) Age	--95% CI--		P(X2) (%)	Sum age (Ma) Age	--95% CI--	
5	1.89E+07	(68)	5.85E+06	(21)	160.8	98.3	275.4	100.0	160.8	98.3	275.4
3	2.20E+07	(79)	6.41E+06	(23)	170.5	107.0	283.5	86.4	166.3	118.6	238.1
14	2.98E+07	(101)	5.31E+06	(18)	275.6	168.4	479.9	23.5	197.9	149.3	262.1
9	5.74E+07	(206)	8.64E+06	(31)	326.0	225.3	488.7	4.9	241.2	191.8	303.0
15	2.25E+07	(54)	3.33E+06	(8)	327.0	159.3	781.4	7.0	248.4	199.3	309.4
7	3.48E+07	(125)	5.01E+06	(18)	339.3	209.6	584.8	6.5	262.6	214.2	321.6
8	5.15E+07	(105)	6.86E+06	(14)	364.8	212.5	680.6	6.2	273.8	225.7	331.9
2	4.51E+07	(162)	5.29E+06	(19)	414.2	261.7	696.1	3.2	291.8	243.4	349.6
11	5.04E+07	(181)	5.85E+06	(21)	418.8	270.6	684.0	1.9	307.7	259.3	364.8
13	4.79E+07	(115)	5.42E+06	(13)	427.7	246.5	812.4	1.8	316.4	268.2	373.1
1	4.48E+07	(161)	5.01E+06	(18)	433.6	271.1	738.9	1.5	327.1	279.1	383.2
6	4.26E+07	(153)	4.18E+06	(15)	491.4	295.9	881.4	0.9	338.8	290.5	395.0
12	7.86E+07	(187)	5.88E+06	(14)	635.6	380.7	1150.8	0.2	357.4	307.8	414.8
4	3.01E+07	(108)	1.95E+06	(7)	721.4	355.7	1732.1	0.1	368.8	318.2	427.1
10	8.02E+07	(288)	4.18E+06	(15)	895.5	553.8	1554.6	0.0	401.5	347.9	462.9
POOL	4.31E+07	(2093)	5.26E+06	(255)				0.0	401.5	347.9	462.9

MEAN URANIUM CONCENTRATION +/-2SE (ppm): 205.8, 26.3

POOLED AGE WITH 68% CONF. INTERVAL(Ma): 401.5, 373.2 -- 431.8 (-28.2 +30.3)
95% CONF. INTERVAL(Ma): 347.9 -- 462.9 (-53.5 +61.5)
REDUCED CHI^2, DEGREES OF FREEDOM: 3.6606, 14
CHI^2 PROBABILITY: 0.0%

CENTRAL AGE WITH 68% CONF. INTERVAL(Ma): 373.2, 330.2 -- 421.6 (-43.0 +48.4)
95% CONF. INTERVAL(Ma): 293.5 -- 473.7 (-79.7 +100.5)
AGE DISPERSION (%): 38.8

CHI^2 AGE WITH 68% CONF. INTERVAL (Ma): 327.1, 301.7 -- 354.7 (-25.4 +27.5)
95% CONF. INTERVAL (Ma): 279.1 -- 383.2 (-48.0 +56.1)
NUMBER AND PERCENTAGE OF GRAINS: 11, 73%

www.manaraa.com

==========ZetaAge Program v. 4.8 (Brandon 1/20/05)==========
DATE/TIME: 07-01-2013/17:41:02 FILENAME: E:\FINALR~1\BR3C.TXT
BR3C, U50Z-25

EFFECTIVE TRACK DENSITY FOR FLUENCE MONITOR (tracks/cm^2): 3.153E+05
RELATIVE ERROR (%): 1.32
EFFECTIVE URANIUM CONTENT OF MONITOR (ppm): 12.30
ZETA FACTOR AND STANDARD ERROR (yr cm^2): 321.90 10.60
SIZE OF COUNTER SQUARE (cm^2): 1.000E-08

------ GRAIN AGES IN ORIGINAL ORDER ------

Grain no.	RhoS (cm^-2)	(Ns)	RhoI (cm^-2)	(Ni)	Squares	U+/-2s	Grain Age	Age (Ma) --95% CI--	
1	2.57E+07	(87)	6.49E+06	(22)	339	253 107	196.5	123.3	328.3
2	5.72E+07	(194)	8.26E+06	(28)	339	322 121	340.7	231.4	521.8
3	2.44E+07	(132)	8.89E+06	(48)	540	347 100	137.8	98.7	195.7
4	4.31E+07	(233)	2.78E+06	(15)	540	108 55	736.5	451.6	1293.2
5	3.17E+07	(171)	4.44E+06	(24)	540	173 70	349.8	230.6	555.7
6	3.57E+07	(121)	1.30E+07	(44)	339	506 152	137.7	97.2	198.9
7	4.19E+07	(142)	4.42E+06	(15)	339	173 88	459.0	275.4	826.2
8	2.09E+07	(71)	8.26E+06	(28)	339	322 121	127.0	81.4	203.9
9	3.16E+07	(107)	6.78E+06	(23)	339	265 109	230.6	147.6	377.3
10	4.81E+07	(163)	5.31E+06	(18)	339	207 96	440.4	275.6	750.1
11	3.48E+07	(118)	6.19E+06	(21)	339	242 104	277.3	175.7	461.2

------ GRAIN AGES ORDERED WITH INCREASING AGE ------

Grain no.	RhoS (cm^-2)	(Ns)	RhoI (cm^-2)	(Ni)	Grain age (Ma) Age	--95% CI--		P(X2) (%)	Sum age (Ma) Age	--95% CI--	
8	2.09E+07	(71)	8.26E+06	(28)	127.0	81.4	203.9	100.0	127.0	81.4	203.9
6	3.57E+07	(121)	1.30E+07	(44)	137.7	97.2	198.9	77.5	133.4	101.2	175.7
3	2.44E+07	(132)	8.89E+06	(48)	137.8	98.7	195.7	95.0	135.2	108.7	168.1
1	2.57E+07	(87)	6.49E+06	(22)	196.5	123.3	328.3	52.2	144.9	118.5	177.0
9	3.16E+07	(107)	6.78E+06	(23)	230.6	147.6	377.3	19.8	157.1	130.4	189.1
11	3.48E+07	(118)	6.19E+06	(21)	277.3	175.7	461.2	3.9	170.9	143.4	203.6
2	5.72E+07	(194)	8.26E+06	(28)	340.7	231.4	521.8	0.1	193.5	164.4	227.8
5	3.17E+07	(171)	4.44E+06	(24)	349.8	230.6	555.7	0.0	209.7	179.5	244.7
10	4.81E+07	(163)	5.31E+06	(18)	440.4	275.6	750.1	0.0	226.4	194.9	262.8
7	4.19E+07	(142)	4.42E+06	(15)	459.0	275.4	826.2	0.0	239.7	207.2	277.1
4	4.31E+07	(233)	2.78E+06	(15)	736.5	451.6	1293.2	0.0	267.1	231.9	307.5
POOL	3.55E+07	(1539)	6.60E+06	(286)				0.0	267.1	231.9	307.5

MEAN URANIUM CONCENTRATION +/-2SE (ppm): 257.5, 31.2

POOLED AGE WITH 68% CONF. INTERVAL(Ma): 267.1, 248.5 -- 287.0 (-18.6 +19.9)
95% CONF. INTERVAL(Ma): 231.9 -- 307.5 (-35.2 +40.4)
REDUCED CHI^2, DEGREES OF FREEDOM: 7.5146, 10
CHI^2 PROBABILITY: 0.0%

CENTRAL AGE WITH 68% CONF. INTERVAL(Ma): 249.4, 212.3 -- 292.9 (-37.1 +43.5)
95% CONF. INTERVAL(Ma): 181.7 -- 341.5 (-67.6 +92.2)
AGE DISPERSION (%): 48.7

CHI^2 AGE WITH 68% CONF. INTERVAL (Ma): 170.9, 156.3 -- 186.9 (-14.6 +16.0)
95% CONF. INTERVAL (Ma): 143.4 -- 203.6 (-27.5 +32.7)
NUMBER AND PERCENTAGE OF GRAINS: 6, 55%

www.manaraa.com